Application of RAPRENOx to Diesel Emission Control

Final Report

by

Technor, Inc.
2374 Research Dr.
Livermore, CA 94550

Principal Investigator

Robert A. Perry

for

Minerals Management Service
Department of Interior

Subcontract No. 85K-SC293V
Martin Marietta Corp.

ABSTRACT

This study investigates the use of RAPRENO$_X$, a non-catalytic selective reduction technology, to reduce nitrogen oxides in exhaust from a diesel fired flow reactor. The flow reactor has been constructed to simulate diesel exhaust in order to test the effects of temperature, exhaust composition and means of injection on the process. Investigations in the flow reactor have led to the development of a continuous HNCO source which is crucial to any commercial application. Material investigations have indicated preferred materials for converting cyanuric acid to isocyanic acid in the presence of excess oxygen. The important new result is that RAPRENO$_X$ can be effectively carried out in diesel exhaust at lower temperatures (<550 C) when the process is enhanced by appropriate chemical injection schemes. A chemical kinetic program developed at Sandia National Laboratories has been used to compare a chemical model to the experimental results. The results of the modeling effort have led to an enhanced understanding of the chemistry and have aided the commercial development. The combined program has resulted in demonstrations of the technology in the exhaust of three Cummins engines; a 4B-3.9 (37 kW) diesel generator set, a 6BT-5.9 (100 kW) diesel generator set, and a KTA-51 (1 MW) diesel generator set. In each engine approximately at least 95% NO_X reduction was obtained.

TABLE OF CONTENTS

LIST OF TABLES

LIST OF FIGURES

1.0 BACKGROUND

Emissions of nitrogen oxides (NO_x, x=1,2) are known to be a major cause of photochemical air pollution. Nitrogen oxides also produce nitric acid when oxidized in the atmosphere, which is considered a major component of acid rain. Diesel applications have been estimated to produce 17% of the nitrogen oxide emission in the U.S. with the largest production being due to prime movers (15%) and stationary power generation (2%). With the major emphasis on meeting the goals of the 1990 Federal Clean Air Act, major restrictions on new sources of nitrogen oxide emissions will be enforced in those areas that presently do not meet federal standards for air quality.

Recently formulated EPA regulations require significant reductions in particulate emissions in diesel trucks and buses. With the current state of combustion technology, engine alterations to reduce particulates will tend to increase NO_x emissions, making simultaneous compliance with particulate and NO_x standards technically very difficult. In addition, developmental low-heat-rejection engines may have inherent tendencies toward high NO_x emissions. Exhaust treatment concepts for NO_x control in diesel engines are thus of great significance.

The need for new NO_x control techniques also has been extended to marine diesel applications. Marine diesels have recently come under severe restrictions in the Southern California Coastal Region, and these restrictions may impact on our nation's ability to drill for oil on offshore platforms. While certain NO_x control strategies exist, their potential application to offshore prime movers is questionable, or at best, expensive. In addition, diesel generators are a potential source of electricity in remote locations, such as offshore oil platforms and isolated islands. The use of a safe, cost-effective way to provide NO_x reduction in diesel applications, operating under a variety of conditions, would help to reduce our dependence on foreign oil, by making offshore oil exploration less costly, while helping to keep the environment clean.

The major goal of this program was to develop the RAPRENO$_x$ process for the removal of nitrogen oxides in diesel exhaust. The patented RAPRENO$_x$ process (Perry 1988, 1989, 1990) works by adding gaseous isocyanic acid to an exhaust gas stream. Isocyanic acid is formed from the thermal decomposition of cyanuric acid, a non-toxic solid material. Reactions of NO and HNCO generate N_2, CO_2 and H_2O. Approximately one mole of isocyanic acid (HNCO) is needed to remove one mole of nitric oxide (NO).

This report describes our evaluation of the effects of temperature, initial NO_x concentration, initial CO concentration, and mode of injection of isocyanic acid on the process. It also briefly addresses questions concerning the use of catalytic materials in diesel exhaust and the selection of materials suitable for

conversion of cyanuric acid to isocyanic acid in highly oxidizing environments. The process was modeled to help us understand the complex chemistry involved in the NO_X reduction scheme. The results from this work have provided the needed expertise to engineer three full-scale demonstration projects. The technical base was used to design prototypes for a 37 kW generator set, a 100 kW generator set, and finally a 1 MW diesel generator set. Our present cyanuric acid (CYA) delivery and control system design has been tested for greater than 250 hours with excellent results (approximately 95% reduction of NO_X while operating from 50-100% load). These projects have shown the commercial feasibility of the process in actual field environments.

2.0 TECHNICAL APPROACH:

A research program consisting of a combination of experimental and modeling efforts was conducted to further characterize, develop, and assess the RAPRENO $_X$ process for NO_X control in diesel exhaust. The major goal of this research was to develop the necessary understanding of the chemistry to evaluate and implement the process. As part of this research effort a number of tasks were undertaken to reach the objective of our first demonstration of NO_X reduction on a diesel engine.

The first task was the construction of a flow reactor which enabled us to simulate combustion phenomenon in a laboratory environment. This multifuel flow reactor was capable of operating over a range of conditions typical of heavy-duty diesel engines. The usable fuels for the flow reactor included conventional diesel fuel and natural gas. A Fourier transform infrared (FTIR) analyzer was used to measure N_2O, CO, CO_2, HNCO, NH_3, and HCN at discrete locations within the flow reactor. In addition, non-dispersive infrared (NDIR) instrumentation was used to measure CO and CO_2 while a chemiluminescent analyzer was used to measure NO_X. This facility is described in detail in section 3.0.

The next major task was to conduct laboratory-scale experiments. Before we were able to conduct these experiments we developed an injection system that pregasified the isocyanic acid prior to injection. After calibrating this system we gathered chemical data in exhaust typical of diesel applications. The following parameters were tested:

1. Exhaust temperature sensitivity
2. Oxygen sensitivity
3. Emissions
4. Cyanuric acid usage
5. Residence time effects
6. Surface enhanced initiation

The experimental results are discussed in section 4.0.

The final task was to model the process as a means to improve our basic

understanding of the process. By comparing the experimental results with the modeled projections we could gain insights to aid in engineering a practical system. We used computational facilities at Sandia National Laboratories for the initial calculations while a version of the Chemkin code was incorporated into a Compaq 386 personal computer at Technor for the majority of the calculations. This modeling effort provided the necessary theoretical framework to implement the chemistry in a commercial diesel generator set. The model will be discussed in section 5.0.

3.0 TEST FACILITY:

The flow diagram of the completed test facility is indicated in Figure 1 while a detailed schematic of the gas analysis system is outlined in Figure 2. The details of the flow reactor are shown in Figure 3.

The flow reactor consists of three main sections: 1) combustion and cooling section, 2) injection section, and 3) test section. Natural gas, or diesel doped with nitrogen containing compounds is burned in the combustion zone. The combustion zone section is nominally 7 inches in diameter and 30 inches long. Gas temperatures leaving the combustion zone section and entering the injection section are controlled by five permanently mounted stainless steel coils that are used to provide course heat extraction and by a series of removable water cooled probes that provide fine temperature control.

Isocyanic acid (HNCO) is injected into the injection section using one 3/8-inch diameter injector. The injector section is a venturi with a 3-inch diameter throat and an increasing exit to match the 8-inch diameter test section. A thermocouple port is located 1 inch above the plane of the injectors.

The test section is 8 inches in diameter and 95 inches long (exit of the injection section to the exit of the flow reactor). Sampling ports are spaced every 19" along the walls of the test section. Additional ports are located across from the sampling ports as shown in Figure 3. These latter ports are used for thermocouple access. The test section has two independent electrically heated sections to help maintain isothermal conditions.

The combustor is fabricated from a castable insulating refractory. The walls are nominally 5 inches thick along the test section. The castable refractory sections are wrapped with 4.5 inches of Kaowool ceramic fiber insulation and the complete unit is housed in a steel casing.

Gas flow to the unit is metered with rotameters. All temperatures are measured with ceramic shielded Pt-Pt 13% Rd thermocouples. A calibration has been established between these thermocouples and a suction pyrometer and the true gas temperature obtained during routine testing using the shielded thermocouples and the correction factor obtained from the suction pyrometer. The suction pyrometer temperature, considered more accurate, should be 60 C higher than the shielded thermocouples.

Residence times in the unit are changed by varying the sampling location at a fixed throughput through the combustor or by varying the combustor throughput. The typical ranges of combustor operating parameters are summarized in Table I.

Table I. Combustor Operating Parameters

	Range	Baseline
Firing Rates:	70 - 350 kBtu/hr	150 kBtu/hr
Combustor Flow Rates:	15 - 70 scfm	22 scfm
Test Section Velocity:	5 - 33 ft/sec	8 ft/sec
Test Section Temps:	400 - 1400 C	600 C
Residence Times:	0.05 - 1.8 sec	1.0 sec
Test Sec. Reynolds No.:	1,000 - 10,000	2,200

Gaseous and solid samples are obtained from the combustor using a water cooled gas quench probe. A thimble separates the solids while the gas sample is transported to the gas analyzers through a heated teflon sample line. The sample is analyzed for O_2, CO_2, CO, and NO_x using the equipment listed in Table II.

Besides the instrumentation listed in Table II, a Mattson Polaris FTIR with a 6 meter multipass gas cell was used to characterize the exhaust. This instrument has a high sensitivity for such gas species as HNCO, N_2O, NH_3, HCN, CO, and CO_2. This system allows for the simultaneous detection of a wide variety of infrared active species with a sensitivity better than 1 ppm in ideal conditions and practical sensitivities of 5-10 ppm in combustion environments. Figure 4 shows calibration plots for HCN and NH_3.

Table II. Gas Analysis Instrumentation

Species	Analyzer	Range*
O_2	Teledyne Model 326RA	0 - 5%
		0 - 10%
		0 - 25%
CO	Horiba Model PIR 2000	0 - 500 ppm
		0 - 1500 ppm
		0 - 2500 ppm
CO_2	Horiba Model PIR 2000	0 - 5%
		0 - 15%
		0 - 25%
NO/NO_x	TECO Model 14BE	0 - 50 ppb
		0 - 100 ppb
		0 - 200 ppb
		0 - 500 ppb
		0 - 1 ppm
		0 - 2 ppm
		0 - 5 ppm
		0 - 10 ppm**

* Selected concentration range. Sensitivity resolution better than 2% full scale.
** Extended to higher ranges using diluted flows with mass flow meters.

4.0 EXPERIMENTAL RESULTS

A major part of this program involved the development of a HNCO source. This was important in order to design an effective injection system using gaseous isocyanic acid instead of solid cyanuric acid. The importance of a gaseous delivery system was predicated by the fact that physical sublimation and chemical conversion of cyanuric acid was rate limiting at low temperatures (< 850 C). Prior attempts to inject cyanuric acid at low temperatures demonstrated that it was not possible to obtain reasonable conversion of cyanuric acid to isocyanic acid at less than 850 C. In order to obtain the best efficiency, and to prevent any unwanted slippage of cyanuric acid, our injection design focused on conversion of cyanuric acid to isocyanic acid prior to injection into the flow reactor. While a continuous variable feed system was our ultimate goal, a continuous feed system was not completed until late in the program, after completing extensive materials testing. Figure 5 shows a schematic of the static HNCO source. We obtained experimental data using this source to evaluate the process with respect to

potential NO_X reduction, effects of co-injection of additives, effects of high oxygen concentrations, and unwanted emissions. Due to engineering problems associated with the design (heat transfer, size and temperature control), the static delivery system could produce approximately 1 gram per minute of HNCO and therefore we were unable to obtain concentrations that were greater than 400 ppm HNCO in the exhaust. This limitation prevented the effective testing of the process at high NO concentration (>500 ppm) in the flow reactor. (This limitation does not now exist.)

The calibration of isocyanic acid concentration as a function of bed temperature for our static delivery system is shown in figure 6. As seen in the figure, the production of isocyanic acid was strongly dependent on the temperature of the cyanuric acid bed. As the temperature was increased above 500 C the production of isocyanic acid became very sensitive to changes in temperature, initial preparation of the isocyanic acid vessel, and a slow flow of air through the vessel. In addition unstable HNCO production was obtained, due to carry over of the cyanuric acid vapor and recondensation. This resulted in plugging of the delivery system. (The problem of increased HNCO production without carry over of cyanuric acid or unwanted byproducts was solved when a continuous delivery system was designed after this project was completed. The material testing provided the needed information to design a continuous delivery systems that could produce up to 300 grams per minute.)

Following the design of a stable reproducible static system, the effect of co-injection of CO with HNCO was investigated. Figure 7 shows the reduction efficiency of NO_X as a function initial CO level and temperature. For an initial NO_X concentration of 505 ppm, a 70-75% reduction in NO_X is obtained at temperatures of 635-760 C. Note that at lower temperatures increasing concentrations of CO are needed to produce significant NO_X reduction. There are two possible explanations for the ability of CO, or other added fuel, to enhance the reduction of NO_X by isocyanic acid. The first explanation is that additional heat is required to promote the decomposition of the isocyanic acid. The second explanation is that the additional radicals or chain carriers are needed at the lower temperature. The fact that no significant temperature rise (>50 C) was associated with the addition of the fuel suggests that radical propagation is required to enhance the process at lower temperatures. Note that as the amount of CO was increased the amount of electrical heat added to maintain isothermal conditions was reduced. Hence, the burning of CO provided the correct radial generation scheme rather than simply providing a higher operating temperature. (These results will be compared to calculations that confirm this theory in section 5.0.) These results are compatible with our understanding of CO flammability limits and suggest the possibility of lowering the operating temperature through the use of fuels with low ignition temperatures. At lower temperatures, more CO is required in order to provide for the necessary radical generation to initiate chain branching.

One important consequence of this result is the apparent trade off

between NO_x reduction and CO production at lower temperatures. Without the addition of sufficient fuel to enhance the burning of the CO in the exhaust residual CO could result at lower temperatures. Any use of alternative additives such as methanol, diesel fuel, or more exotic "enhancers" such as peroxides or oxidizers will result in unburned CO production at lower temperatures (<600 C). This prediction is based upon the results of this testing and CO flammability limits. With increased temperatures and time, or the use of a CO catalyst the residual CO may be greatly reduced or eliminated. (Note that testing to date in diesel engines indicates that the CO may be reduced below the initial CO found in untreated exhaust with appropriate design.) From these results appropriate enhancement of the homogeneous process was predicted to occur at low temperatures by co-injection of a small percentage of CO or a hydrogen producing fuel. (Confirmation of this result will be discussed in section 6.0 for the actual diesel testing.)

Besides CO and NO_x, we investigated additional unwanted emissions. The production of N_2O, NH_3, and HCN were not observed in our testing in the multifuel reactor where a detection limit of 20 ppm N_2O, 10 ppm NH_3, and 2 ppm HCN was estimated based upon our prior calibration for these gases. Based upon our improved understanding of the process, it is somewhat surprising that no N_2O was observed in these experiments at temperatures less than 650 C. (Testing in actual diesel exhaust has shown that less than 200 ppm of N_2O is produced with the final concentration of N_2O being influenced by the particular exhaust configuration.) Work is continuing in our diesel testing to confirm and quantify these results. Prior work [Plane 1987] has suggested that at temperatures greater than 600 C N_2O may be greatly reduced by heterogeneous surface reactions. This may explain the inability to observe N_2O in the flow reactor and the effects of reactor design on the final N_2O produced.

The second part of the experimental testing involved an effort to generate the homogeneous reactions using surface catalyzed initiation. It was felt that a catalyst could be used to decompose the isocyanic acid either prior to injection or while in contact with the exhaust. While these experiments were under way, Siebers and Caton (1988) reported successful use of iron oxide to enhance the process at lower temperatures. An effort was made to test both iron oxide and a Rh/Alumina oxide substrate in the flow reactor. Unfortunately, experimental difficulties prevented effective testing and we were unable to reproduce the results of Siebers and Caton. Figure 8 shows the test reactor that was used to test the catalytic activity. While we were attempting to catalytically enhance NO_x reduction, we discovered that in oxidizing environments some materials, such as iron oxide, had a propensity to produce NO_x with the added cyanuric acid at elevated temperatures. We began an effort to characterize materials that would be compatible with cyanuric acid in air. (Air was a practical medium to transport gaseous HNCO.)

The material compatibility test utilized a quartz tube containing porcelain

Table III: Material Compatibility Testing with Cyanuric Acid and Air

	Material	Amount (g)	Amount (mm^2)	CYA (g/s)	Air Flow (SCFM)	Temps (c)	Results
1.	Control Test	-	-	2	2.05	750	Obtained 2000 ppm HNCO
2.	White Binder	14.9	3,200	2	2.4	735	Short run. Saw significant amounts of NO_X (<.3 ppm NO_X).
3.	Grey Glue	10.8	1,900	2	2.4	740	Good run, lasted 1 hour, little NO_X, good efficiency (1800 ppm HNCO)
4.	Inconel 600	12.9	1,1575	2	2.4	715-820	Low NO_X except after 780 C (HNCO > 1800 ppm)
5.	Inconel 750X	24.5	3,924	2	2.4	680-750	Low efficiency - Ran >1.2 hours, low NO_Xuntil 750 C
6.	Brass	46.2	6,038	2	2.05	750-800	Extremely bad material- HNCO = 1150 ppm, NO_X = 1.2 ppm
7.	Hastelloy	7.5	1,205	2	2.05	730	Good efficiency, still low NO_X, ran > 1.5 hours
8.	Hastelloy	5.7	6,000	2	2.05	745	Produced > 5 ppm NO_X, Otherwise good efficiency.
9.	Monel	1.3	1,300	2	2.05	730-845	Above 760 C produced NO_X
10.	Monel	5	20,000	2	2.05	688-775	NO_X produced

	Material	Amount (g) (mm^2)	CYA (g/s)	Air Flow (SCFM)	Temp (C)	Results
11.	Nickel	20 1,285	2	2.05	750	Very low NO_X
12.	Copper	12 2,640	2	2.04	720-800	Very high NO_X even at low temperature
13.	Copper	12 2,640	2	2.04	720	Very high NO_X
14.	Nichrome Wire	2 3,770	2	2.05	740-860	Very low NO_X
15.	Molybdenum	17 2,065	2	2.05	800	No NO_X until extra Mo was added on top of test reactor.
16.	Molybdenum	17 2,065	2	2.05	730-800	Demonstrated temperature dependence of NO_X levels. Also NO_X increased when nichrome was added to top
17.	Fe Shavings	5 18,000	2	2.05	680	Poor efficiency, lots of NO_X
18.	Titanium	4.9 2,700	2	2.05	730-800	No NO_X after 800 C. Ti produces little or no NO_X.
19.	Titanium (New)	5.7 6,200	2	2.05	830-900	Good efficiency and very little NO_X

packing material and known amounts of test materials. Cyanuric acid powder was introduced into the heated tube in a controlled manner. The materials were evaluated for their effect on HNCO and NO production as a function of temperature. Table III lists the materials tested for compatibility with cyanuric acid in air. At higher temperatures and in the presence of air, brass and stainless steel produced low levels of NO_x when contacted with cyanuric acid. Under low oxidizing conditions, and at lower temperatures, it was possible to produce HNCO efficiently in a brass or stainless steel vessel. Under oxidizing conditions, and at higher delivery throughput, where higher temperatures were required, the scaled delivery systems using brass failed to provide a clean source of isocyanic acid. Fortunately, materials other than steel or brass were found to be compatible with CYA, and a continuous delivery system could produce high levels of isocyanic acid without unwanted byproducts.

5.0 MODELING RESULTS:

Technor has established a modeling capability by implementing a detailed chemical kinetic model developed at Sandia National Laboratories. The proposed mechanism, which presently contains 101 reactions, is outlined in Table IV. The chemical kinetic code is available from Sandia National Labs [Kee 1980]. Using Chemkin the time history of a homogeneous reaction, equivalent to a diffusion-free plug-flow reactor is calculated. These calculations are normally carried out for two second reaction times, although at higher temperatures the chemistry is normally complete in less than 100 ms. Note that the use of a time dependent calculation does not correctly represent the actual experimental application in a diesel exhaust where recirculation and mixing effects may be more important. Nevertheless, these calculations allowed for the extrapolation of limited experimental results and they aided in understanding the best approach toward extending results to temperatures below 625 C.

The calculations were performed based upon a matrix of possible initial conditions. We chose initial conditions that included 100, 500, 1,000 and 5,000 ppm NO_x, either 5% or 10% O_2 , either 200, 1,000, or 5,000 ppm CO, and HNCO/NO ratio of 1 or 2. The results are outlined in Figures 9-24. Important insights into more complex systems may be deduced from the results. One important result from the model is the apparent shift in temperature with the addition of CO to the exhaust. This is in agreement with our experimental results. Figures 25-27 shows a comparison between theory and our experimental results. While the model predicts a somewhat better reduction than observed in our flow reactor, it is important to note that the results accurately reproduce observations in our diesel generator sets, where mixing was not considered to be an important limitation and better control of the injection of isocyanic acid was implemented. The model does predict the general trend of requiring additional CO (or fuel) at temperatures below 650 C. Note that the results in Figure 25-27 were calculated

Table IV: Reaction Mechanism Rate Coefficients In Form $k = AT^N \exp(-E/RT)$.
(Units are moles, cubic centimeters, seconds, Kelvins and calories/mole.)

#	Reaction	Reference	A factor	N	E
1	$H+O_2 = O+OH$	(MILLER 81)	5.1E16	-0.82	16510
2	$H_2+O = H+OH$	(MILLER 77)	1.8E10	1.0	8830
3	$H_2+OH = H_2O+H$	(DIXON-LEWIS 77)	1.2E09	1.3	3630
4	$OH+OH = H_2O+O$	(COHEN 79)	6.0E08	1.3	0
5	$H+OH+M = H_2O+M$ H_2O /5.0/	(MILLER 89)	1.6E22	-2.0	0
6	$H+H+M = H_2+M$ H_2O /0.0/ CO_2 /0.0/ H_2 /0.0/	(DIXON-LEWIS 81)	1.0E18	-1.0	0
7	$H+H+H_2 = H_2+H_2$	(DIXON-LEWIS 81)	9.2E16	-0.6	0
8	$H+H+H_2O = H_2+H_2O$	(DIXON-LEWIS 81)	6.0E19	-1.25	0
9	$H+H+CO_2 = H_2+CO_2$	(DIXON-LEWIS 81)	5.5E20	-2.0	0
10	$H_2+O_2 = OH+OH$	(MILLER 77)	1.7E13	0.0	47780
11	$HO_2+H = H_2+O_2$	(MILLER 89)	1.25E13	0.0	0
12	$H+O+M = OH+M$ H_2O /5.0/	(MILLER 89)	6.2E16	-0.6	0
13	$HO_2+H = OH+OH$	(MILLER 89)	1.4E14	0.0	1073
14	$HO_2+O = OH+O_2$	(MILLER 89)	1.4E13	0.0	1073
15	$HO_2+OH = H_2O+O_2$	(MILLER 89)	7.5E12	0.0	0
16	$HO_2+HO_2 = H_2O_2+O_2$	(TROE 69)	2.0E12	0.0	0
17	$H_2O_2+M = OH+OH+M$	(BAULCH 72)	1.3E17	0.0	45500
18	$H_2O_2+H = HO_2 + H_2$	(BAULCH 72)	1.6E12	0.0	3800
19	$H_2O_2+OH = H_2O+HO_2$	(BAULCH 72)	1.0E13	0.0	1800
20	$CO+O+M = CO_2+M$	(MILLER 89)	6.17E14	0.0	3000
21	$CO+O_2 = CO_2+O$	(MILLER 89)	1.6E13	0.0	41000
22	$CO+OH = CO_2+H$	(BAULCH 74)	1.5E07	1.3	-760
23	$CO+HO_2 = CO_2+OH$	(ATRI 77)	5.8E13	0.0	22930
24	$HCO+M = CO+H+M$	(SCHECKER 69)	1.6E14	0.0	14700
25	$HCO+H = CO+H_2$	(DIXON-LEWIS 81)	4.0E13	0.0	0
26	$HCO+O = CO+OH$	(BROWNE 69)	3.0E13	0.0	0
27	$HCO+O = CO_2+H$	(WARNATZ 84)	3.0E13	0.0	0
28	$HCO+OH = CO+H_2O$	(DIXON-LEWIS 81)	5.0E1	0.0	0

29	$HCO+O_2 = CO+HO_2$	(VEYRET 84)	3.3E13	-0.4	0
30	$N_2H_2+M = NNH+H+M$	(MILLER EST 83)	5.0E16	0.0	50000
31	$N_2H_2+H = NNH+H_2$	(MILLER EST 83)	5.0E13	0.0	1000
32	$NNH = N_2+H$	(PERRY/ 2/27/87)	1.0E07	0.0	0
33	$N_2H_2+OH = NNH+H_2O$	(PERRY 10/17/86)	7.0E13	0.0	0
34	$NNH+H = N_2+H_2$	(MILLER 81)	3.7E13	0.0	3000
35	$NNH+NO = N_2+HNO$	(MILLER 81)	5.0E13	0.0	0
36	$NH_3+M = NH_2+H+M$	(MILLER 81)	1.4E16	0.0	90600
37	$NH_3+H = NH_2+H_2$	(MICHAEL 1985)	6.36E05	2.39	10171
38	$NH_3+O = NH_2+OH$	(PERRY 84a)	2.1E13	0.0	9000
39	$NH_3+OH = NH_2+H_2O$	(SALIMIAN 84)	2.04E6	2.04	566
40	$NH_2+H = NH+H_2$	(ROOSE 81)	6.9E13	0.0	3650
41	$NH_2+O = NH+OH$	(DRANSFELD 84)	6.8E12	0.0	0
42	$NH_2+O = HNO+H$	(DRANSFELD 84)	6.6E14	-0.5	0
43	$NH_2+OH = NH+H_2O$	(BRANCH 82)	4.5E12	0.0	2200
44	$NH_2+N = N_2+H+H$	(PHILLIPS 84)	7.2E13	0.0	0
45	$NH_2+NH = N_2H_2+H$	(MILLER 83)	5.0E13	0.0	0
46	$NH_2+NO = NNH+OH$	(MILLER 83)	8.8E15	-1.25	0
47	$NH_2+NO = N_2+H_2O$	(MILLER 83)	3.8E15	-1.25	0
48	$NH+H = N+H_2$	(MILLER 89)	1.0E14	0.0	0
49	$NH+O = NO+H$	(MILLER 83)	2.0E13	0.0	0
50	$NH+OH = HNO+H$	(MILLER 83)	2.0E13	0.0	0
51	$NH+OH = N+H_2O$	(ROOSE 77)	5.0E11	0.5	2000
52	$NH+O_2 = HNO+O$	(MILLER 83)	1.0E13	0.0	12000
53	$NH+O_2 = NO+OH$	(MILLER 89)	7.6E10	0.0	1530
54	$NH+NO = N_2O+H$	(MILLER 89)	2.4E15	-0.8	0
55	$NH+N = N_2+H$	(MILLER EST 84)	3.0E13	0.0	0
56	$N+O_2 = NO+O$	(BAULCH 73)	6.4E09	1.0	6280
57	$N+OH = NO+H$	(HOWARD 81)	3.8E13	0.0	0
58	$N+NO = N_2+O$	(MONAT 79)	3.3E12	0.3	0
59	$N+CO_2 = NO+CO$	(AVRAMENKO 67)	1.9E11	0.0	3400
60	$NO+HO_2 = NO_2+OH$	(HOWARD 80)	2.1E12	0.0	-480
61	$NO_2+M = NO+O+M$	(BAULCH 73)	1.1E16	0.0	66000
62	$NO_2+H = NO+OH$	(SEE MILLER 81)	3.5E14	0.0	1500
63	$NO_2+O = NO+O_2$	(BAULCH 73)	1.0E13	0.0	600
64	$HNO+M = H+NO+M$	(BAULCH 73)	1.5E16	0.0	48680
	H_2O /10.0/				
	H_2 /2.0/				
	O_2 /2.0/				

	N_2 /2.0/				
65	HNO+H = H_2+NO	(BAULCH 73)	5.0E12	0.0	0
66	HNO+OH = NO+H_2O	(BAULCH 73)	3.6E13	0.0	0
67	N_2O+M = N_2+O+M	(MONAT 77)	1.6E14	0.0	51600
68	N_2O+H = N_2+OH	(BAULCH 73)	7.6E13	0.0	15200
69	N_2O+O = NO+NO	(BAULCH 73)	1.0E14	0.0	28200
70	N_2O+O = N_2+O_2	(BAULCH 73)	1.0E14	0.0	28200
71	HCN+O = CN+OH	(PERRY 84b)	2.7E09	1.58	26600
72	HCN+O = NCO+H	(THORNE 86)	1.4E04	2.64	4980
73	HCN+O = NH+CO	(THORNE 86)	3.5E03	2.64	4980
74	HCN+OH = CN+H_2O	(MILLER 86)	1.5E13	0.0	10929
75	HCN+OH = HOCN+H	(MILLER 86)	9.2E12	0.0	15000
76	HCN+OH = HNCO+H	(MILLER 86)	4.8E11	0.0	11000
77	HCN+CN = C2N_2+H	(SZEKELY 86)	2.0E13	0.0	0
78	CN+O = CO+N	(LOUGE 84)	1.8E13	0.0	0
79	CN+OH = NCO+H	(HAYNES 77)	6.0E13	0.0	0
80	CN+H_2 = HCN+H	(WAGNER 85)	3.0E05	2.45	2237
81	CN+O_2 = NCO+O	(LOUGE 84)	5.6E12	0.0	0
82	NCO+OH = NO+CO+H	(MILLER EST 84)	1.0E13	0.0	0
83	OH+HNCO = H_2O+NCO	(TULLY 88)	2.65E12	0.0	5540
84	HNCO = NH+CO	(MERTENS 88)	1.14E16	0.0	86800
85	NCO+H_2 = HNCO+H	(PERRY 85)	8.6E12	0.0	9000
86	NCO+N = N_2+CO	(LIFSHITZ EST 80)	2.0E13	0.0	0
87	NCO+NO = N_2O+CO	(PERRY 85)	1.0E13	0.0	-390
88	HOCN+H = HNCO+H	(EST)	1.0E13	0.0	0
89	HNCO+H = NH_2+CO	(MILLER EST 84)	2.0E13	0.0	3000
90	C2N_2+O = NCO+CN	(LOUGE 1985)	4.6E12	0.0	8880
91	O+HNCO = NH+CO_2	(TULLY 88)	3.25E12	0.0	10300
92	NH_2+HNCO = NH_3+NCO	(MERTENS 88)	5.0E12	0.0	6200
93	NH+HNCO = NH_2+NCO	(MERTENS 88)	3.0E13	0.0	23700
94	C2N_2+OH = HOCN+CN	(PHILLIPS 79)	1.9E11	0.0	2900
95	NCO+M = N+CO+M	(LOUGE 84)	3.1E16	-0.5	48000
96	CN+NO_2 = NCO+NO	(EST)	3.0E13	0.0	0
97	CN+N_2O = NCO+N_2	(EST)	1.0E13	0.0	0
98	NCO+H = NH+CO	(LOUGE EST 84)	5.0E13	0.0	0
99	NCO+O = NO+CO	(MILLER 89)	2.0E13	0.0	0
100	H+O_2+M = HO_2+M	(MILLER 89)	3.6E17	-0.72	0
	H_2O /18.6/				
	CO_2 /4.2/				
	H_2 /2.9/				

CO /2.1/
O_2 /0.0/
N_2 /1.3/

101	$H+O_2+O_2 = HO_2+O_2$	(SLACK 77)	6.7E19	-1.42	0

---

for constant temperature and pressure, so that only the effect of the chemistry, not temperature rise, would be important in the NO_X reduction.

Another important observation is that the location of optimum temperature shifts to higher temperatures with higher initial NO_X concentration. This is best explained by the inhibiting effect that high concentrations of isocyanic acid have on the flammability of the exhaust mixture. It is difficult to oxidize isocyanic acid at low temperatures. The addition of fuel to the exhaust results in better NO_X reduction at lower temperatures by enhancing the production of radicals. This results in a more efficient usage of CYA per mole of NO_X reduced.

It is possible to predict the ability to extend the process to lower temperatures (less than 650 C) by evaluating the flammability of the gas mixture that would result from the addition of a fuel. It is difficult to predict quantitatively this limit using the reaction set that comprises this model. (Complex fuels, such as diesel fuel, are not easily modeled with a chemical kinetic code.) However, this model has given us additional confidence in predicting the low temperature limit, and in suggesting the best procedure to extend the low temperature limit.

At temperatures greater than 800 C kinetic constraints are less important than equilibrium constraints. Thus, reactions, which at low temperatures play a minor role, i.e (91), (95), and (99), become more important and help to drive the chemistry toward equilibrium. One important consequence is that additional CYA is required to reduce NO_X levels at these higher temperatures. In addition, at higher temperatures isocyanic acid begins to resemble other SNCR techniques, in that predictions of NO_X reduction can be based on equilibrium calculations with good results.

From the model it is apparent that the reaction

$$H + O_2 \rightarrow O + OH \qquad (1)$$

is a very important chain branching reaction providing the needed reactive radicals to carry out the chemistry. The competing termination reaction

$$H + O_2 + M \rightarrow HO_2 + M \qquad (100)$$

becomes important at lower temperatures and effectively scavenges the hydrogen atoms, when the appropriate fuel is not added to enhance the flammability of the mixture at lower temperatures. Both in the model and in experiments this reaction is manifested in the production of NO_2 from reaction (60) when insufficient

radicals are produced to activate the HNCO. (This effect is also seen even when HNCO is not added.) When fuel is added, a competing reaction resulting in H_2O_2 production and additional chain branching extends these results to 370 C. This is a good example of where the model may be used to predict the effect of adding fuel to lower the low temperature limit. While the model does not address the "cool" flame chemistry directly, the reactions responsible for the low temperature limit may be assessed and used to engineer better systems.

The reaction

$$OH + HNCO \rightarrow NCO + H_2O \qquad (83)$$

provides the important rate limiting reaction producing the active species NCO. Reaction (87) then provides for the conversion of NO to N_2O which ultimately is reduced to N_2 by reaction with hydrogen, hydroxyl radical, or by thermal decomposition of N_2O.

While the reaction set chosen for our model is based upon the most reliable estimates of elementary reactions there are certain inherent limitations in the proposed model. The model over predicts the amount of N_2O resulting from the process at low temperatures. This may suggest that alternative pathways are available for reaction (87). One reaction that was not considered during the course of these calculations was the reaction

$$NCO + NO \rightarrow OCNNO \rightarrow N_2 + CO_2 \qquad (87b)$$

Although, this reaction was not included in our model as an elementary reaction, if reaction (87b) is important, it may explain our inability to predict the concentration of N_2O. (This reaction has been proposed by a group from Aerodyne [Zahniser 1986] although its importance must still be substantiated.)

An important conclusion based upon this model is that the reaction

$$H + HNCO \rightarrow NH_2 + CO \qquad (89)$$

is not considered to be as important as once believed in oxidizing environments (5-10% O_2). In more complex exhaust systems, where a fuel has been added to enhance the effectiveness of the process, reaction (89) may become more important at lower temperatures (<500 C) and lower oxygen concentrations (<3%). As a consequence of these calculations, it is believed that ammonia, which would be formed from the sequence of reaction (89) followed by the reverse of reaction (39) is formed only if adequate radical enhancement has not been utilized to augment the injection scheme. This accounts for the fact that no ammonia is formed from the process at lower temperatures when fuels are injected.

In summary, though the use of this model certain key items become

apparent. The first important result is that NO_X reduction is best obtained at lower temperatures with "combustible" mixtures. The addition of a fuel, such as hydrogen, carbon monoxide, propane, or diesel fuel that will ignite at lower temperatures provides the best means of assuring significant NO_X reduction at low temperatures. (The experimental work is continuing in actual diesel applications where the fuel is chosen from less expensive and more practical candidates such as diesel, propane, natural gas, etc.) The most important limitation appears to be the flammability of the "combustible". We have presently extended our choice of fuel to include propane and #2 fuel oil. The limitation involved with using hydrocarbon fuels appears to be in the residual CO concentration that results at lower temperatures. The residual CO is inversely related to the temperature, oxygen concentration, and residence time. Higher oxygen concentration allows for better combustion to occur at lower temperatures while longer times (> 1 sec) and higher temperatures (> 650 C) result in CO levels that are less than the 150 ppm level found in untreated diesel exhaust. If both low CO and low temperatures are required, an oxidizing catalyst must be used to consume the CO.

6.0 DIESEL DEMONSTRATIONS:

Following this program, work has progressed toward demonstrations of the technology in three engine applications. Figures 28-30 show experimental results from our successful diesel demonstrations on 37 kWatt, 100 kWatt and 1 MWatt generator sets operating at three different loads. By applying our understanding of the process to these systems we have been able to achieve 95% reduction of NO_X with one mole of HNCO to one mole of NO_X and no increase in CO output. These results included the co-injection of propane or diesel fuel as the hydrogen/CO source. Without the use of a heat exchanger to minimize fuel consumption we have been able to reduce our need for additional diesel to approximately 10-15% of the normal fuel required for engine operation under full load conditions. While a fuel was added to the exhaust, we were unable to detect any residual hydrocarbons in the exhaust. This result was not unexpected considering the low CO level that was measured, i.e. the hydrocarbon fuel was consumed prior to CO burnout.

In all of the demonstrations, CYA is fed continuously into a sublimation/converter assembly prior to being injected into the exhaust. One important consideration is the need to insure adequate mixing of the added isocyanic acid and fuel in the exhaust. Heated air is used to inject the gaseous isocyanic acid into the exhaust stream. The injection point for the isocyanic acid is diametrically opposed to the fuel/air injection point and near the exhaust manifold in both the 37 kWatt and 100 kWatt generator sets. This particular design causes both injected streams to be mixed by the exhaust within 10 pipe diameters downstream from the injection point. The 1 MWatt generator set has a

duel exhaust which provided effective mixing of the isocyanic acid with a single injection nozzle. The exhaust is then expanded into a reaction chamber providing for approximately one second reaction time. This reaction time minimized needed fuel to consume CO produced from the addition of the fuel. It also allowed for the most effective use of the isocyanic acid. A portion of the exhaust is collected by a heated sample system and analyzed for NO_x, CO, CO_2, O_2, and infrared active byproducts, such as NH_3, HCN, and N_2O.

In conclusion, by combining previous laboratory results, a chemical kinetic model, and simple mixing theory, RAPRENO$_x$ has been effectively implemented on a commercial scale. These results suggest a practical procedure for utilizing the technology in commercial applications.

7.0 TECHNICAL AND ECONOMIC SUMMARY FOR DIESEL APPLICATIONS:

Based upon the recent prototype demonstration and the first commercial installation, a summary of benefits and associated cost for a 4,000 hp marine diesel are listed below. These estimates are based upon best available information as of December 1990. The cost of cyanuric acid is based upon chemical supplier quotes. The lowest cost ($.09/lb) is from a pilot scale production facility now operating in Europe by a major chemical producer while the highest cost ($.39/lb) is a quoted domestic price as of summer of 1990. We have used the format suggested in the report by L. W. Philp (1988), updating the section with regard to amount of NO_x reduction and fuel needed to achieve NO_x reduction using the RAPRENO$_x$ process.

Successful application of the RAPRENOX process to stationary heavy duty engines offers the following benefits:

- Reduction of 95% of NO_x from exhaust without affecting engine performance requirements. We have obtained a level of 45 ppm NO_x at 8% oxygen in a 1 MWatt generator set which started at 1150 ppm NO_x.
- Easily retrofitable to diesel applications with flexible operating conditions. Not effected by soot or sulfur dioxide.
- No increase in CO emissions are observed.
- No slippage of ammonia or isocyanic acid is observed.
- Allows heavy duty engine design emphasis to be redirected from minimizing NO_x emissions formation to optimizing commercial attributes, i.e., performance, durability, reliability, reduced complexity, and costs. This includes a 4-6% improvement in fuel economy for diesel engines. (This does not include cost of fuel that must be used to enhance the process. This cost must be calculated on an individual basis based upon operating conditions.)
- Provides a cost effective method for reducing NO_x emissions from stationary engine exhausts compared to other available methods. Table V shows an updated cost estimate for RAPRENO$_x$ while table VI shows an updated cost/benefit comparison for applicable NO_x control technologies.

The cost estimates for the operation of the RAPRENO$_X$ system on the 4000 hp shaft output stationary diesel engine are derived using the following assumptions and calculations to be consistent with estimate by L. W. Philp (1988):

- o Assumptions:
  - 4,000 hp engine shaft output
  - 9 grams NO_x/hp-hr. in exhaust
  - 95% NO_x removal efficiency
  - $0.70/gallon diesel fuel
- o Cost Calculations:
  - 4000 hp = 2980 kW
  - 4000 hp x 9 grams NO_x/hp-hr. = 36,000 grams NO_x/hr.
  - 36 kg NO_x/hr. = 79.4 lbs. NO_x/hr. = 695,000 lbs. NO_x/yr.
  - 79.4 lbs. NO_x/hr. x 1 lb. cyanuric acid /1 lb. NO_x = 79.4 lbs. cyanuric acid/hr.
  - 79.4 lbs. cyanuric acid/hr. x $0.09/lb. cyanuric acid = $7.15/hr.
  - $7.15/hr. /2982.8 kW = 2.4 mills/kW-hr.
  - Capital cost for fully optimized and volume produced delivery system is estimated to be $35,700 for a 1MWatt shaft output engine application ($35.70/kW). This cost should be the same for a 4,000 hp engine.

Table V. Comparison of Different NO_x Control Technologies for Diesel Engines (Based on cost estimate by L. W. Philp (1988).)

Basis
4000 hp
95 percent NO_x removal efficiency
Annual NO_x Reduction @ 95% = 165 tons

Estimate	High	Low
Installed Cost ($35/hp)	$140,000	$140,000
Annual Operating Cost @ 50% Annual Load Factor:		
Reagent Cost @ $0.09/lb and 1 lb/lb NO_x		$ 30,000
Reagent Cost @ $0.39/lb and 1 lb/lb NO_x	$129,000	
Additional Fuel @ 10% of fuel input and $0.70/ gallon	$ 58,000	$ 58,000
Other Operating & Maintenance @ 3% of FCI	$ 4,000	$ 4,000
Capital Charges @ 20%	$ 28,000	$ 28,000
Annual TOTAL	$ 219,000	$120,000

Table VI. Summary of Cost Estimates for Different NOx Control Technologies

	Annual NOx Reduction (tons)	Installed Cost (thousand $)	Annual Cost (thousand $)	Cost/NO_x Reduced (thousand $/ton)
Selective Catalytic Reduction	139	600	176	1.27
Selective Non-Catalytic Reduction	104	140	171	1.64
RAPRENO$_x$	165	140	120-219	0.73-1.33

In conclusion, the use of the RAPRENOX process for NO_x control provides a cost effective method for reducing NO_x emissions from stationary engine exhaust compared to other methods. It is possible to obtain better than 90% NO_x reduction for diesel engines operating over the range of load conditions 50-100%. This process should be also well suited to marine diesel applications, where a constant load exists during operation of ship or generator set. Progress to date suggest that the process should be more effective than selective catalytic reduction and easily installed in retrofit applications.

8.0 FUTURE WORK

Work is continuing on implementing the technology in both the 100 kW and 1 MWatt turbocharged generators. The challenges that are presently being solved include transient load following and extension of the process to lower temperatures (<390 C). Long term durability testing (>300 hours of operation) has been completed on an effective delivery system suitable for marine diesel applications. In addition, efforts are continuing to better understand the conditions that result in nitrous oxide production, and to minimize or eliminate this potentially unacceptable emission. These efforts have been encouraging to date and successful commercialization of the process is expected during 1991. The first sales of the process have already been made, demonstrating its new acceptance as a viable pollution control procedure.

9.0 REFERENCES

Atri, G. M., Baldwin, R.R., Jackson D., and Walker, R. W., *Combust. Flame* **30**, 1 (1977).

Avramenko, L. I., and Krasnen'kov, V. M., *Izv. Akad. Nauk SSSR, Ser. Khim.*, 501, (1967).

Baulch, D. L., and Drysdale, D. D., Horne, D. G., and Lloyd, A. C., *Evaluated Kinetic Data for High Temperature Reactions,* **Vol 1**, Butterworth, (1972).

Baulch, D. L., and Drysdale, D. D., Horne, D. G., and Lloyd, A. C., *Evaluated Kinetic Data for High Temperature Reactions,* **Vol 2**, Butterworth, (1973).

Baulch, D. L., and Drysdale, D. D., *Combustion and Flame* **23**, 215 (1974).

Branch, M. C., Kee, R. J., and Miller, J. A., *Comb. Sci. Techn.* **29**, 147 (1982).

Browne, W. G., Porter, R. P., Verlin, J. D., and Clarke, A. H., *12th. Symp. (Int.) Comb.* ,1035 (1969).

Cohen, N., and Westberg, K., unpubl. work, 1979.

Dixon-Lewis, G., Williams, D.J., *Comprehensive Chemical Kinetics*,**17** (C. H. Bamford and C. F. Tipper, Eds.) 1977.

Dixon-Lewis, G., *Phil. Trans. R. Soc. Lond.*, **A303**, 181 (1981).

Dransfeld, P., Hack, W., Kurzke, H., Temps, F., and Wagner, H. Gg., *20th Symp. (Int.) Comb.*, 655 (1985).

Haynes, B. S., *Combust. Flame* **28**, 81 (1977) and **28**, 113 (1977).

Howard, M. J., Smith I. W. M., *J. Chem. Soc. Faraday Trans. 2*, **77**, 997 (1981).

Howard, C. J., *J. Am. Chem. Soc.* 6937, (1980).

Kee, R. J., Miller, J. A., and Jefferson, T. H. Sandia Report SAND80-8003.

Louge, My., and Hanson, R. K. WSS/CI 84-35, (1984a).

Louge, M. Y., and Hanson, R.K., *Int. J. Chem. Kin.* **16**, 231 (1984b).

Louge, M. Y., and Hanson, R. K., and Bowman, C. T., *20th Symp. (Int.) Comb.*, 665 (1985).

Michael, J. V., Sutherland, J. W., and Klemm, R. B., *Int. J. Chem. Kin.* **17**, 315 (1985).

Miller, J. A., and Kee, RJ., *J. Phys. Chem.* **81**, 2534 (1977).

Miller, J. A., *J. Chem. Phys.* **84** , 5120 (1981).

Miller, J. A., Smooke, M.D., Green, R.M., and Kee, R. J., *Comb. Sci. Techn.* **34**, 149 (1983).

Miller, J. A. and Melius, C. F. , *21st Symp. (Int.) Comb.,* (1986).

Miller, J. A. and Bowman, C. T., *Prog. Energy Comb. Sci.* **15**, 287 (1989).

Monat, J. P., Hanson, R.K., Kruger, C. H., *Symp. Int. Combust. Proc.* **17**, 543 (1979).

Perry, R. A., *Chem. Phys. Letts.* **106**, 223 (1984).

Perry, R. A., and Melius C. F., *Twentieth Symp. (Int.) on Comb.*, 639 (1984).

Perry, R. A., *J. Chem. Phys.* **82**, 5485 (1985).

Perry, R. A., U. S. Patents 4,731,231, 4,800,068, 4,886,650, and 4,908,193 (1988, 1989, 1990).

Philp, L. W. "*Offshore Operations NO_X Control Development Program*" Prepared for Minerals Management Service, Department of Interior by Arthur D. Little Inc. (1988).
Phillips, L. F., *Combust. Flame* **35**, 233 (1979).
Plane, J. M.C., *J. Phys. Chem.* **91**, 6552 (1987).
Phillips, L. F., and Whyte, R.A., *Chem. Phys. Letts.* **102**, 451 (1984).
Roose T. R., Hanson, R. K., and Kruger, C. H., *Proceedings of the Eleventh Intern. Shock Tube Symp.*, Univ. of Washington Press, Seattle, Washington, 245 (1977).
Roose T. R., PhD Thesis, Stanford Univ., (1981).
Salimian, S., Hanson, R. K., and Kruger,C. H., *Int. J. Chem. Kin.* **16**, 725 (1984).
Siebers, D. L. and Caton J. A., Presented at Fall Meeting of Western States Section Combustion Institute,WSS/CI 88-66, Dana Point, California (1988).
Schecker, H. G., and Jost, W., *Ber. Bunsenges. Phys. Chem.* **73**, 521 (1969).
Slack, M. W., *Combus. Flame* **28**, 241 (1977).
Szekely, A., Hanson, R. K., and Bowman, C. T., *20th Symp. (Int.) Comb.*, 647 (1985).
Tully, F. P., Perry, R. A., Thorne, L. R. and Allendorf, M. D., *Twenty-second Symp. (Int.) on Comb.*, The Combustion Institute, Pittsburgh. 1101, (1989).
Thorne, L. R., Branch, M. C., Chandler, D. W., Kee, R. J. and Miller, J. A., *21st Symp. (Int.) Comb.*, (1986).
Troe, J., *Ber. Bunsenges. Phys. Chem.*, **73**, 946 (1969).
Veyret, B., and Leslaux, R., *J. Phys. Chem.* **85**, 1918 (1981).
Wagner, A. F., and Bair, R. A., *Int. J. of Chem. Kin.* **18**, 473 (1986).
Warnatz, J. Combustion Chemistry (W. C. Gardiner, Ed.), Springer, (1984).
Zahniser, M., Presented at EPA Workshop on N_2O Emission from Combustion, Durham, N.C. (1986).

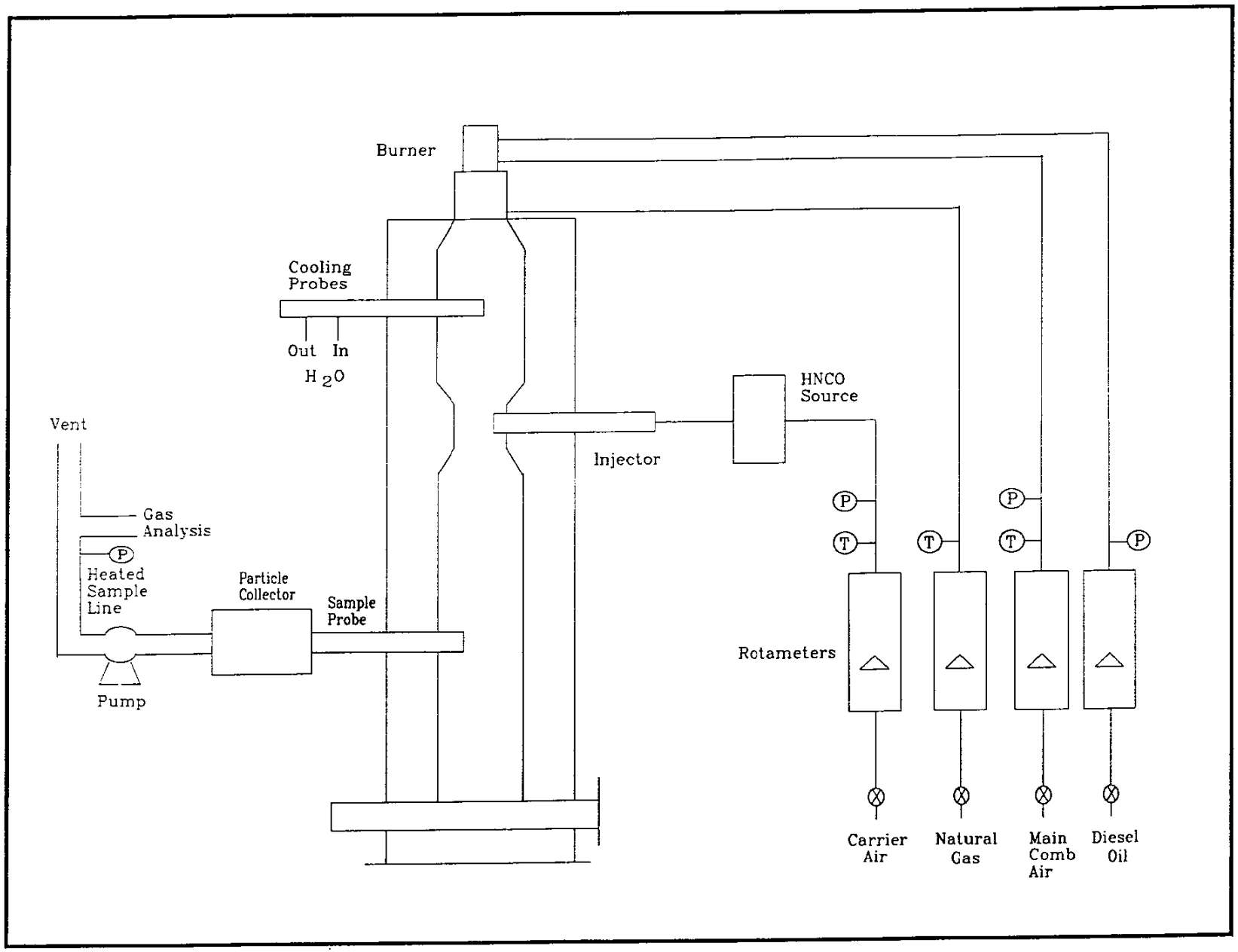

Figure 1. Overall system schematic.

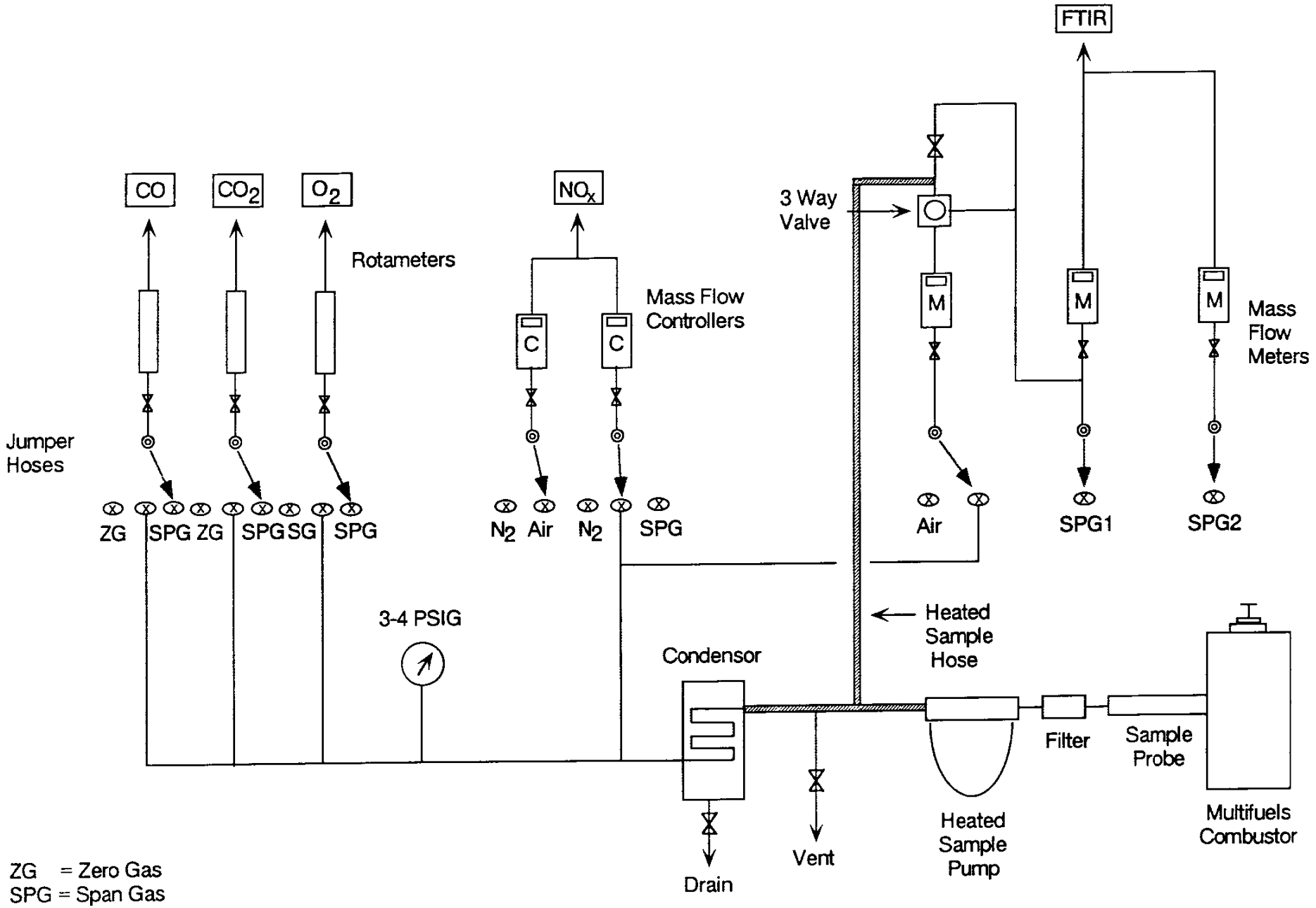

Figure 2. Gas analysis system.

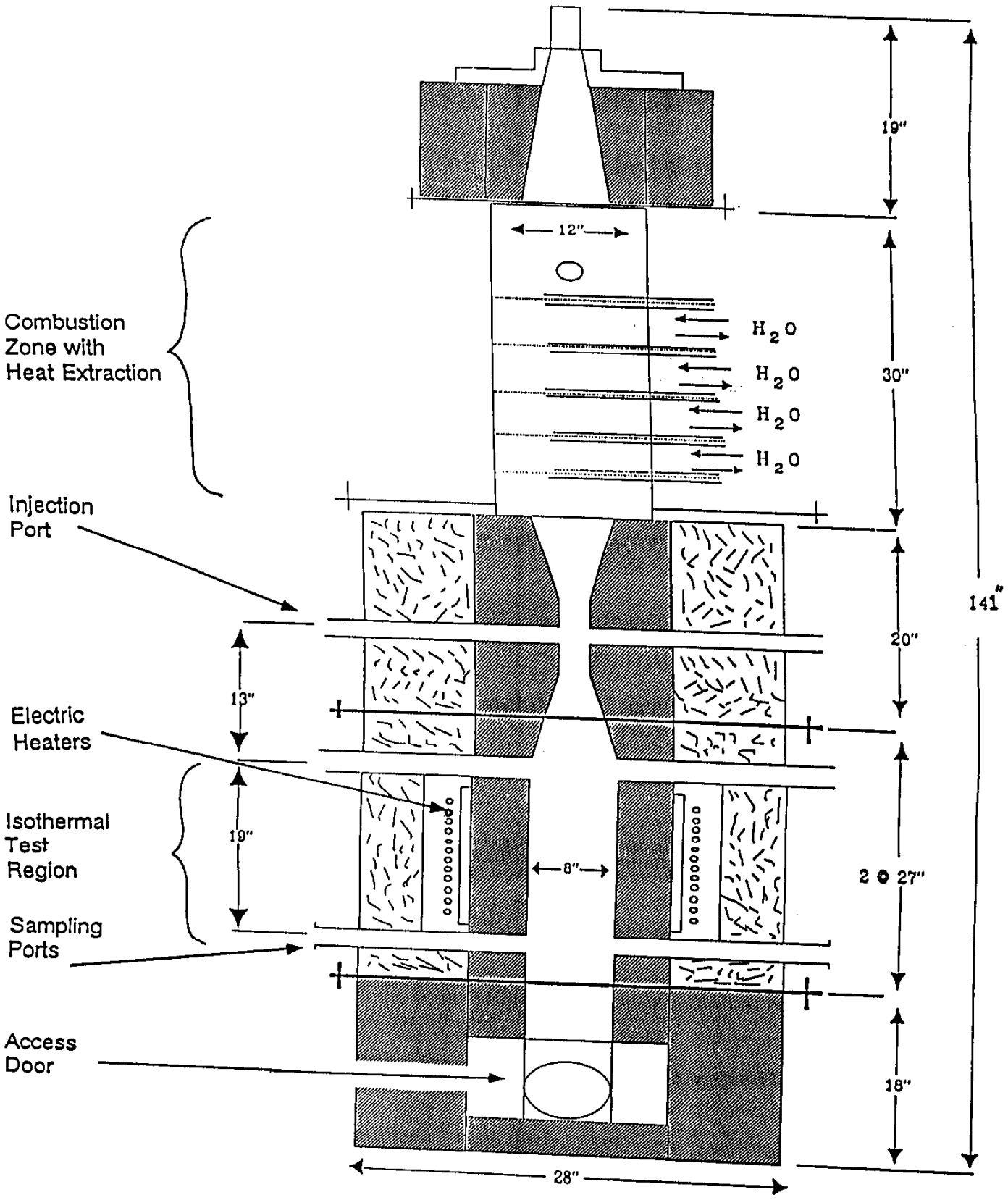

Figure 3. Multifuel flow reactor.

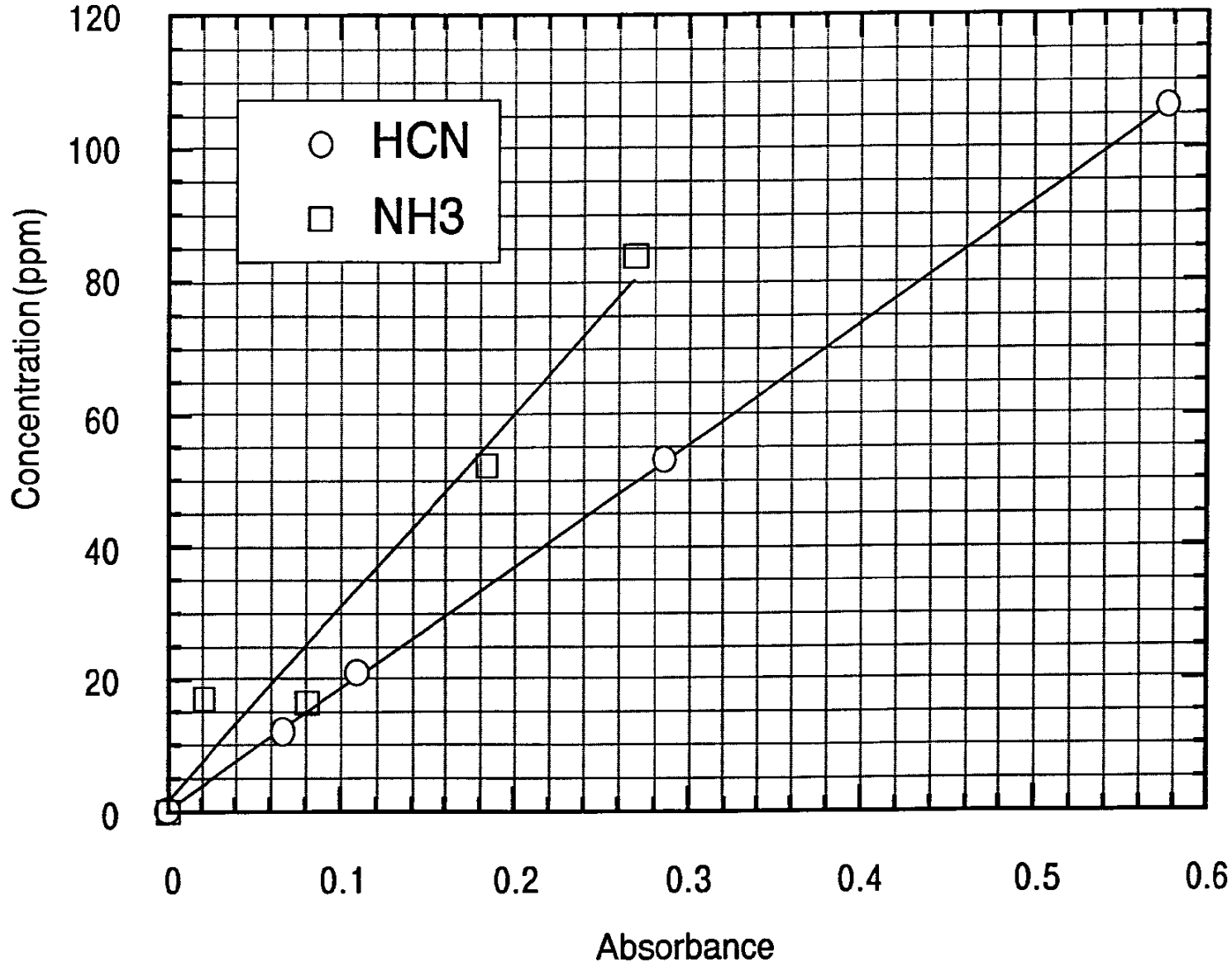

Figure 4. Calibration plot of hydrogen cyanide and ammonia concentration as a function of absorbance.

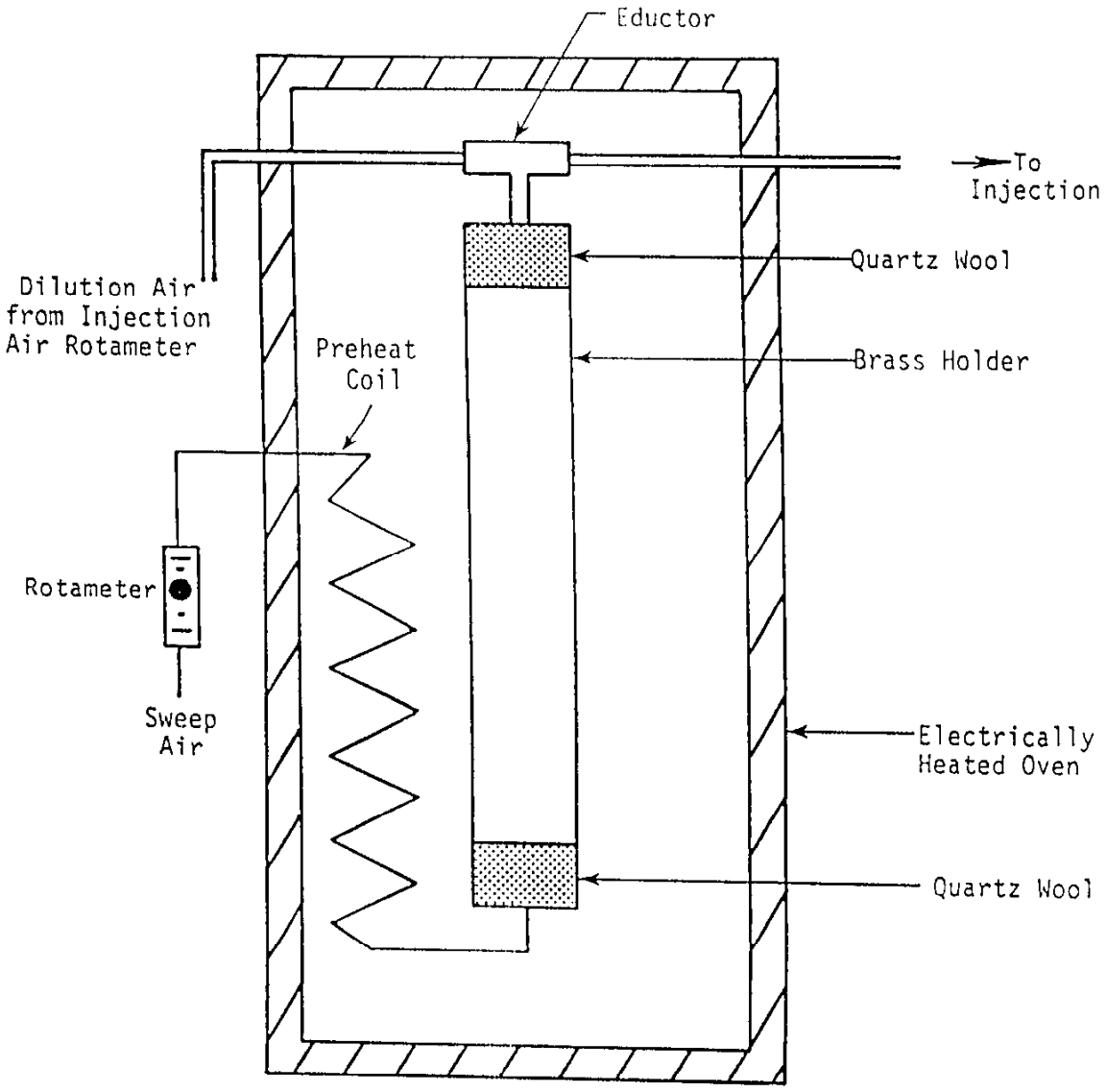

Figure 5. Apparatus used to predecompose cyanuric acid.

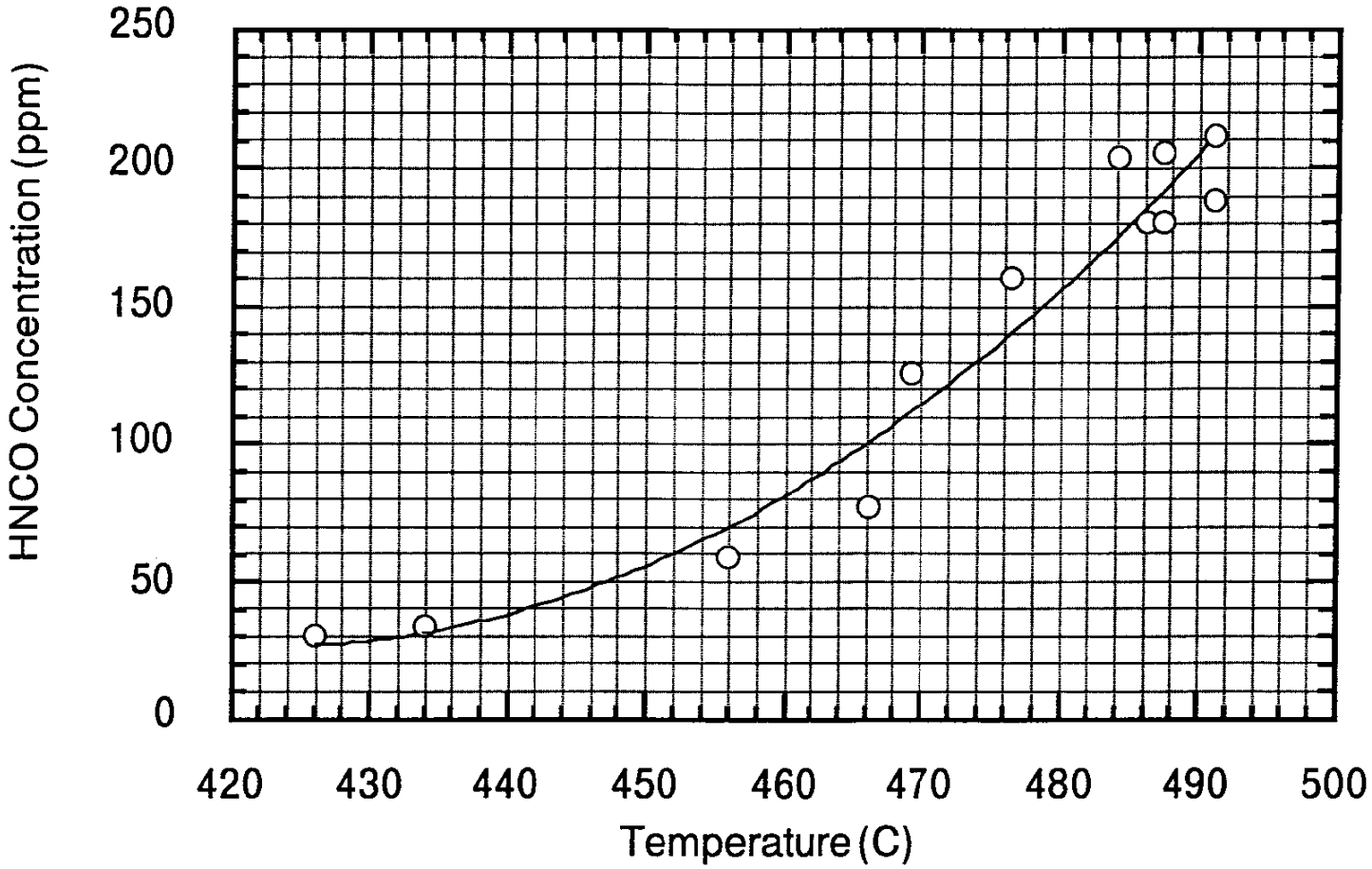

Figure 6. Concentration of isocyanic acid in exhaust as function of bed temperature.

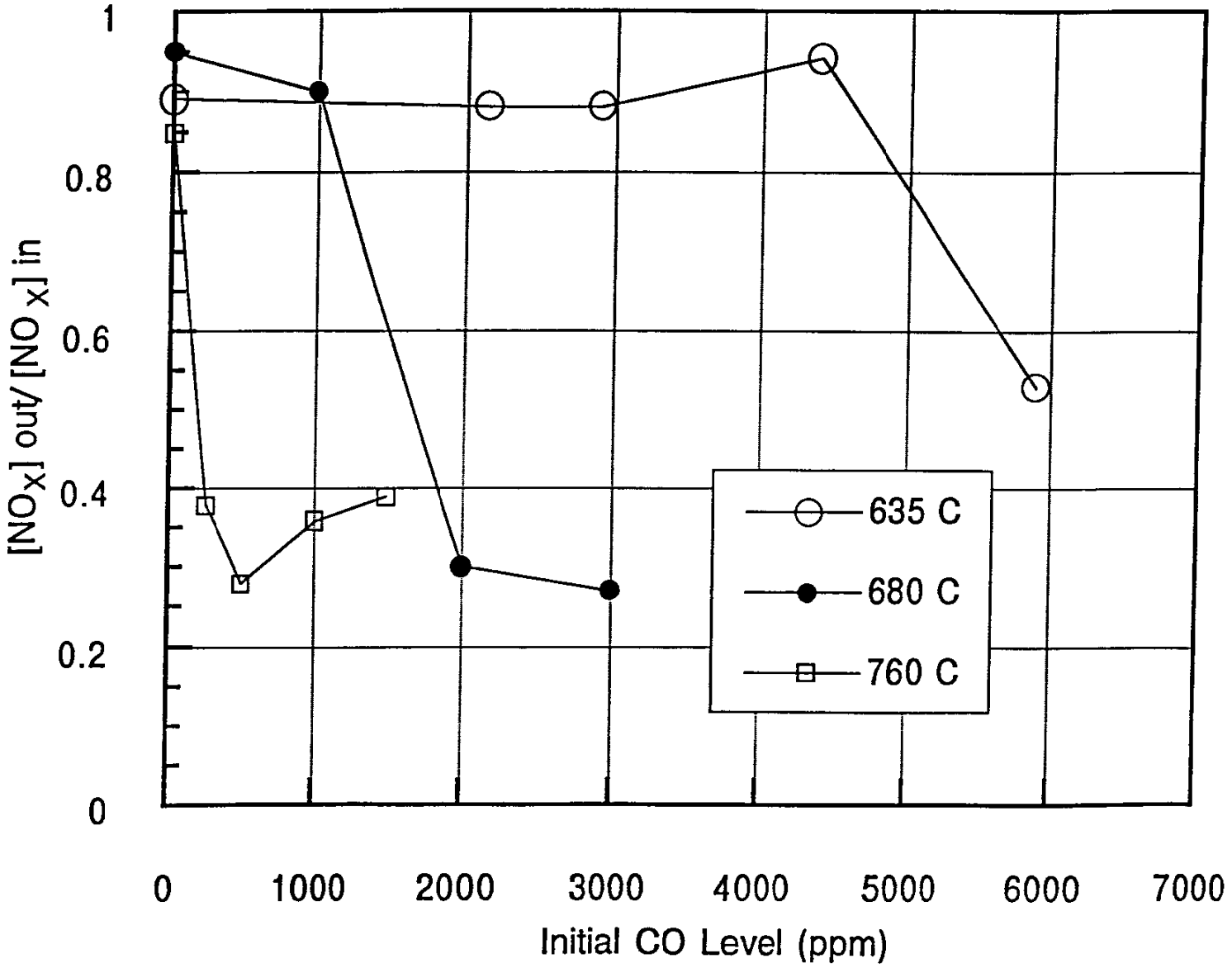

Figure 7. Effect of temperature and carbon monoxide concentration on reduction efficiency ($(NO_X)_i = 505$ ppm).

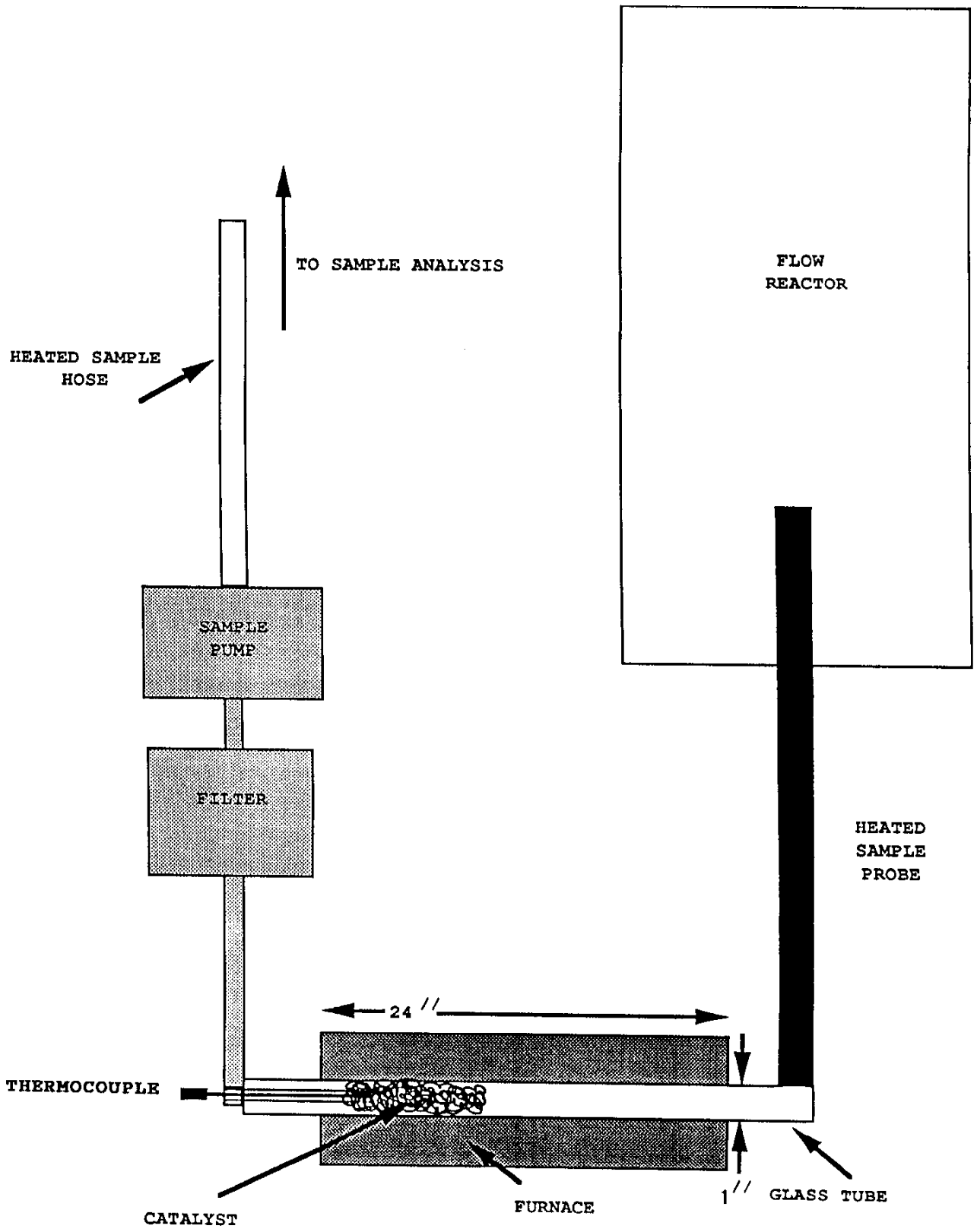

Figure 8. Test reactor used to test effect of surface composition on catalytic effects.

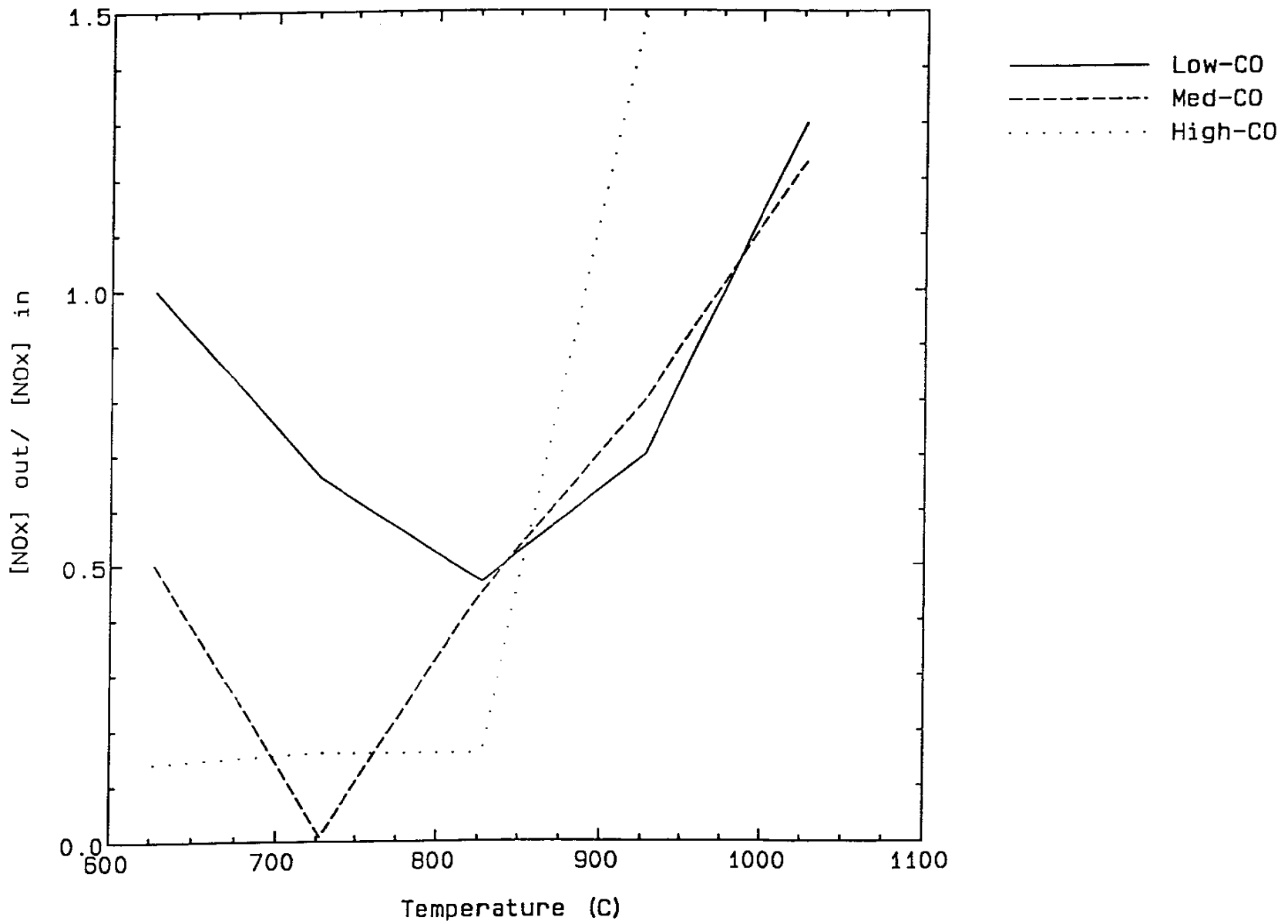

Figure 9. Calculated NO_x reduction efficiency as a function of temperature for selected initial condition: 5% O_2, 100 ppm NO, HNCO/NO = 1. Initial CO conditions selected include low CO = 200 ppm, medium CO = 1000 ppm, and high CO = 5000 ppm.

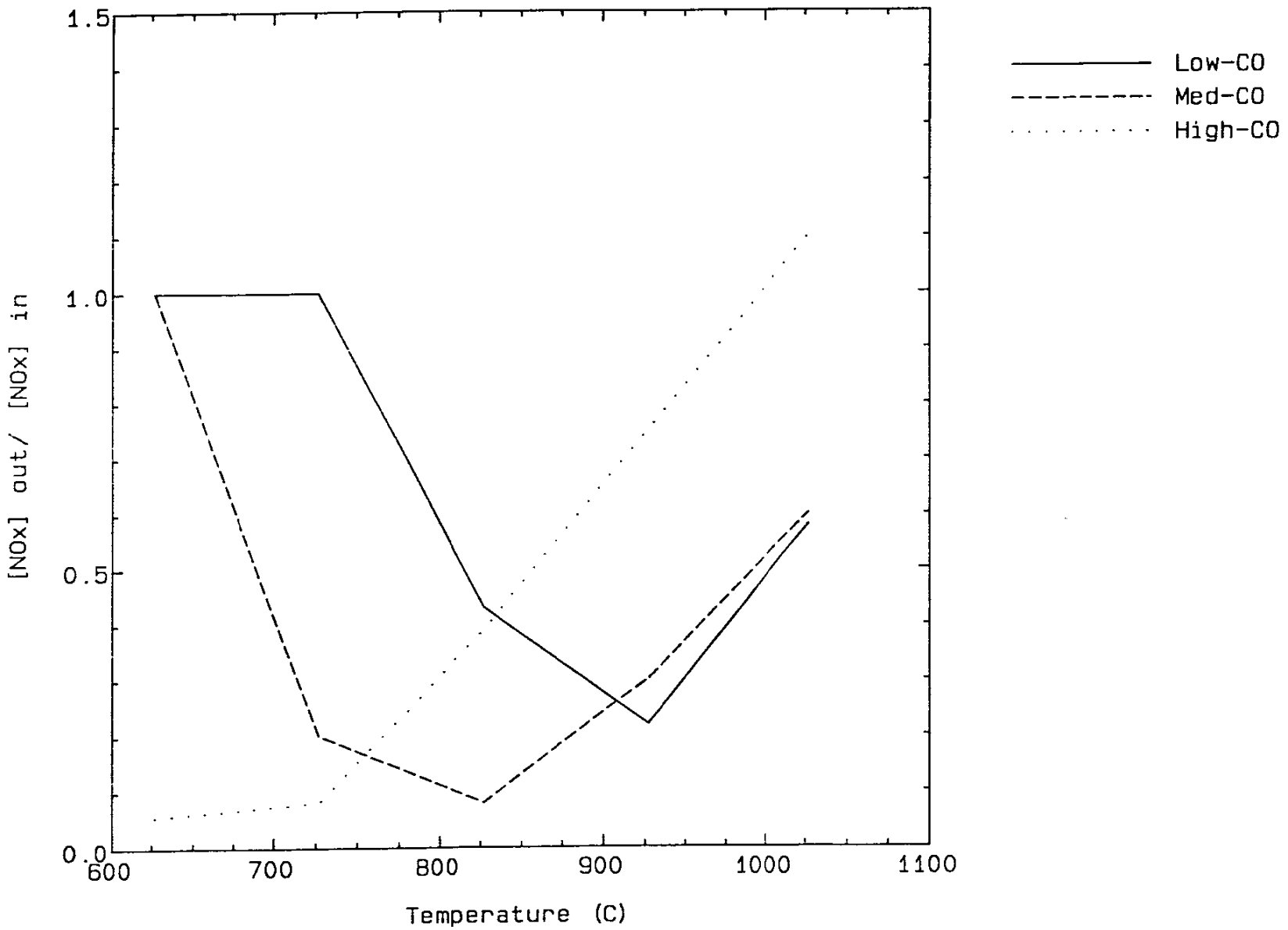

Figure 10. Calculated NO_x reduction efficiency as a function of temperature for selected initial condition: 5% O_2, 500 ppm NO, HNCO/NO = 1. Initial CO conditions selected include low CO = 200 ppm, medium CO =

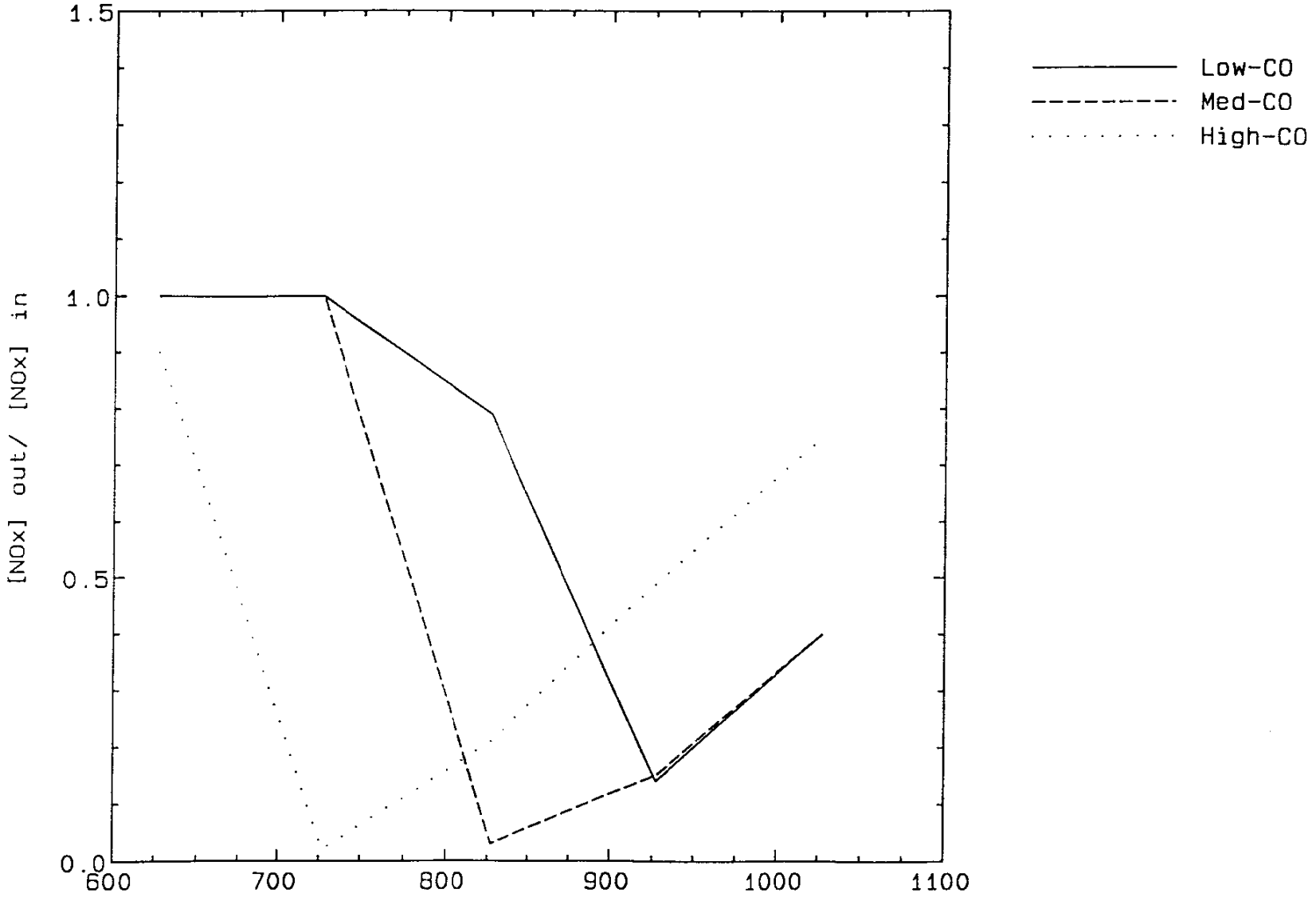

Figure 11. Calculated NO_x reduction efficiency as a function of temperature for selected initial condition: 5% O_2, 1000 ppm NO, HNCO/NO = 1. Initial CO conditions selected include low CO = 200 ppm, medium CO = 1000 ppm, and high CO= 5000 ppm.

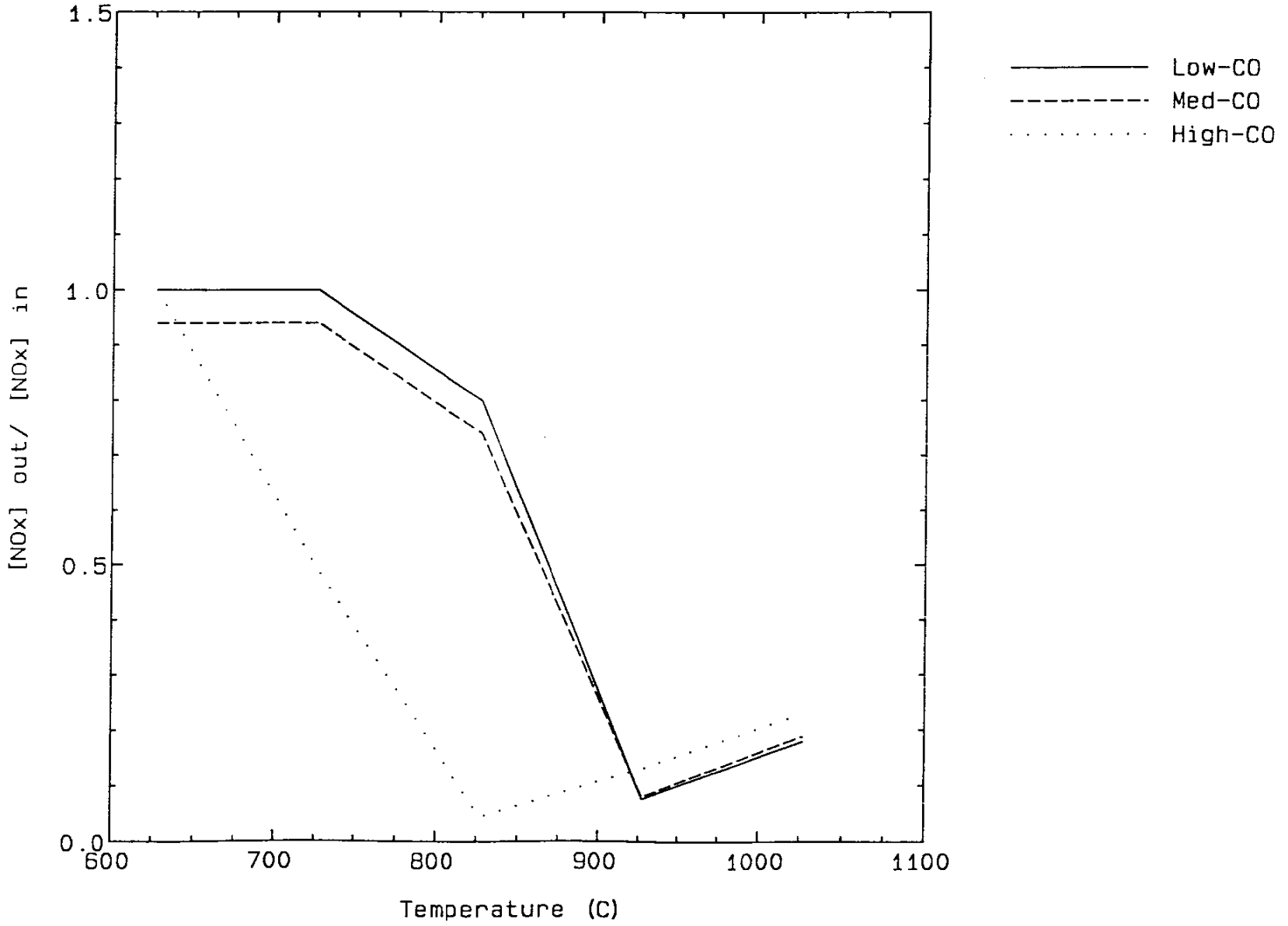

Figure 12. Calculated NO_x reduction efficiency as a function of temperature for selected initial condition: 5% O_2, 5000 ppm NO, HNCO/NO = 1. Initial CO conditions selected include low CO = 200 ppm, medium CO = 1000 ppm, and high CO= 5000 ppm.

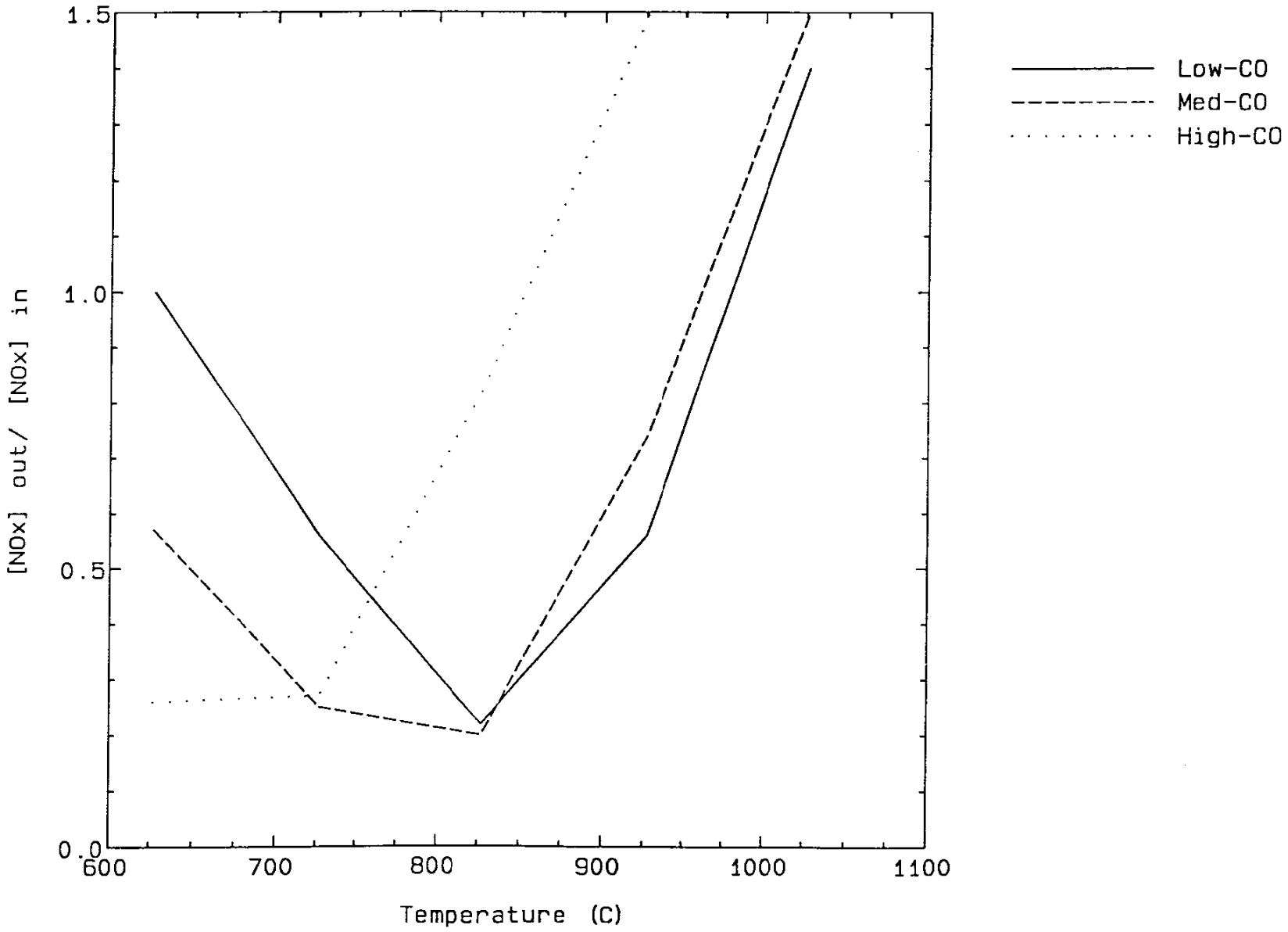

Figure 13. Calculated NO_x reduction efficiency as a function of temperature for selected initial condition: 5% O_2, 100 ppm NO, HNCO/NO = 2. Initial CO conditions selected include low CO = 200 ppm, medium CO = 1000 ppm, and high CO= 5000 ppm.

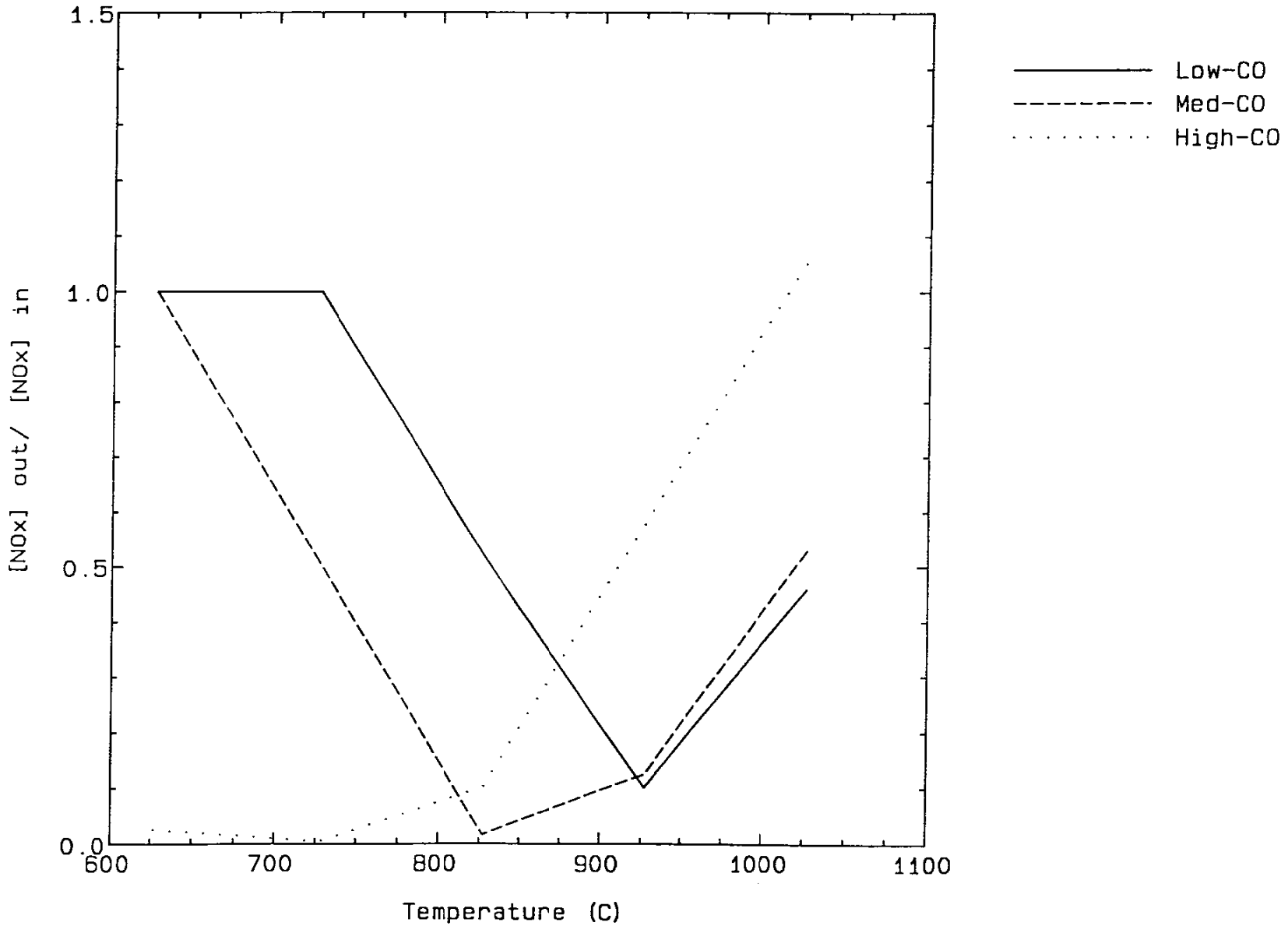

Figure 14. Calculated NO_x reduction efficiency as a function of temperature for selected initial condition: 5% O_2, 500 ppm NO, HNCO/NO = 2. Initial CO conditions selected include low CO = 200 ppm, medium CO = 1000 ppm, and high CO= 5000 ppm.

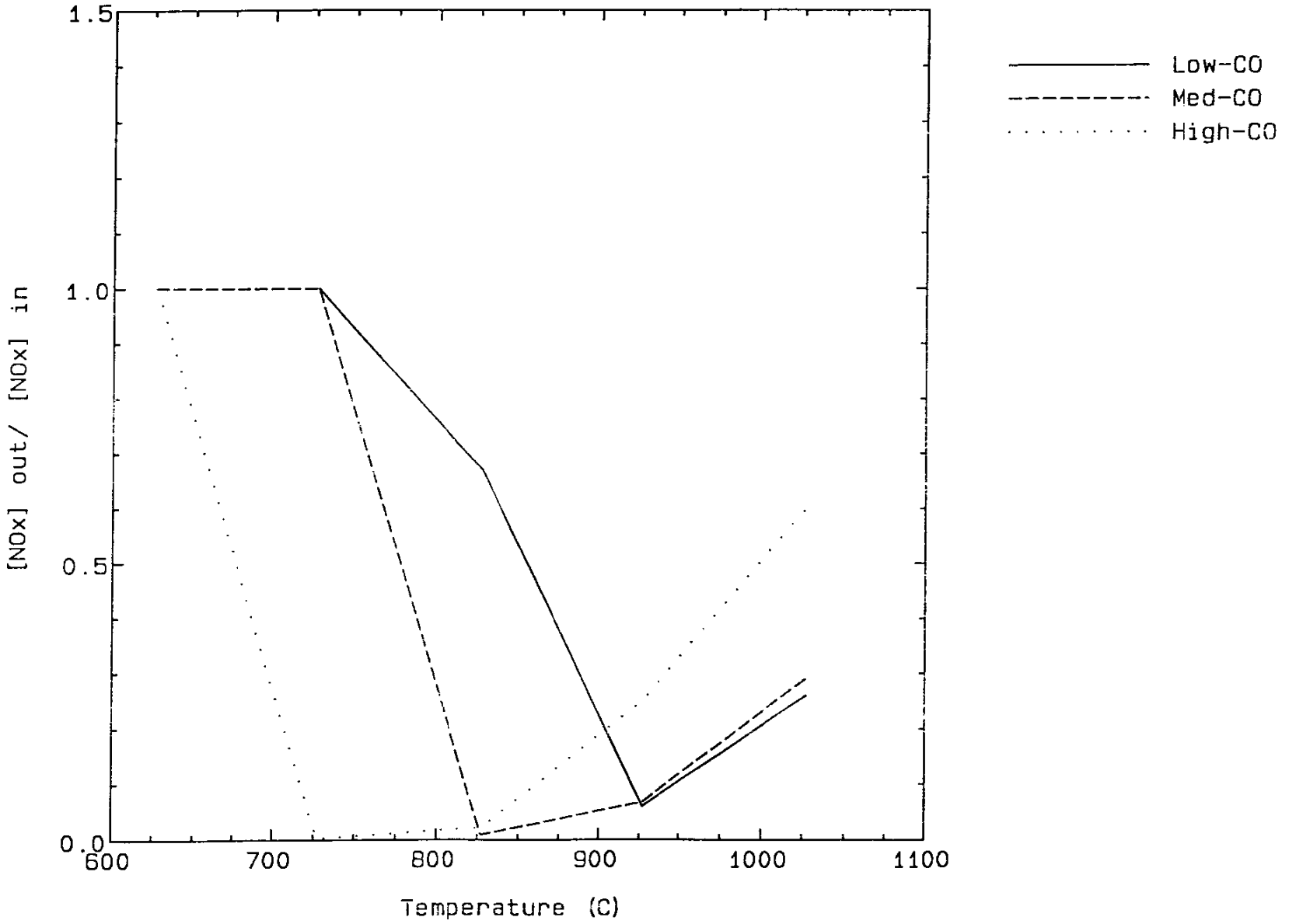

Figure 15. Calculated NO_x reduction efficiency as a function of temperature for selected initial condition: 5% O_2, 1000 ppm NO, HNCO/NO = 2. Initial CO conditions selected include low CO = 200 ppm, medium CO = 1000 ppm, and high CO= 5000 ppm.

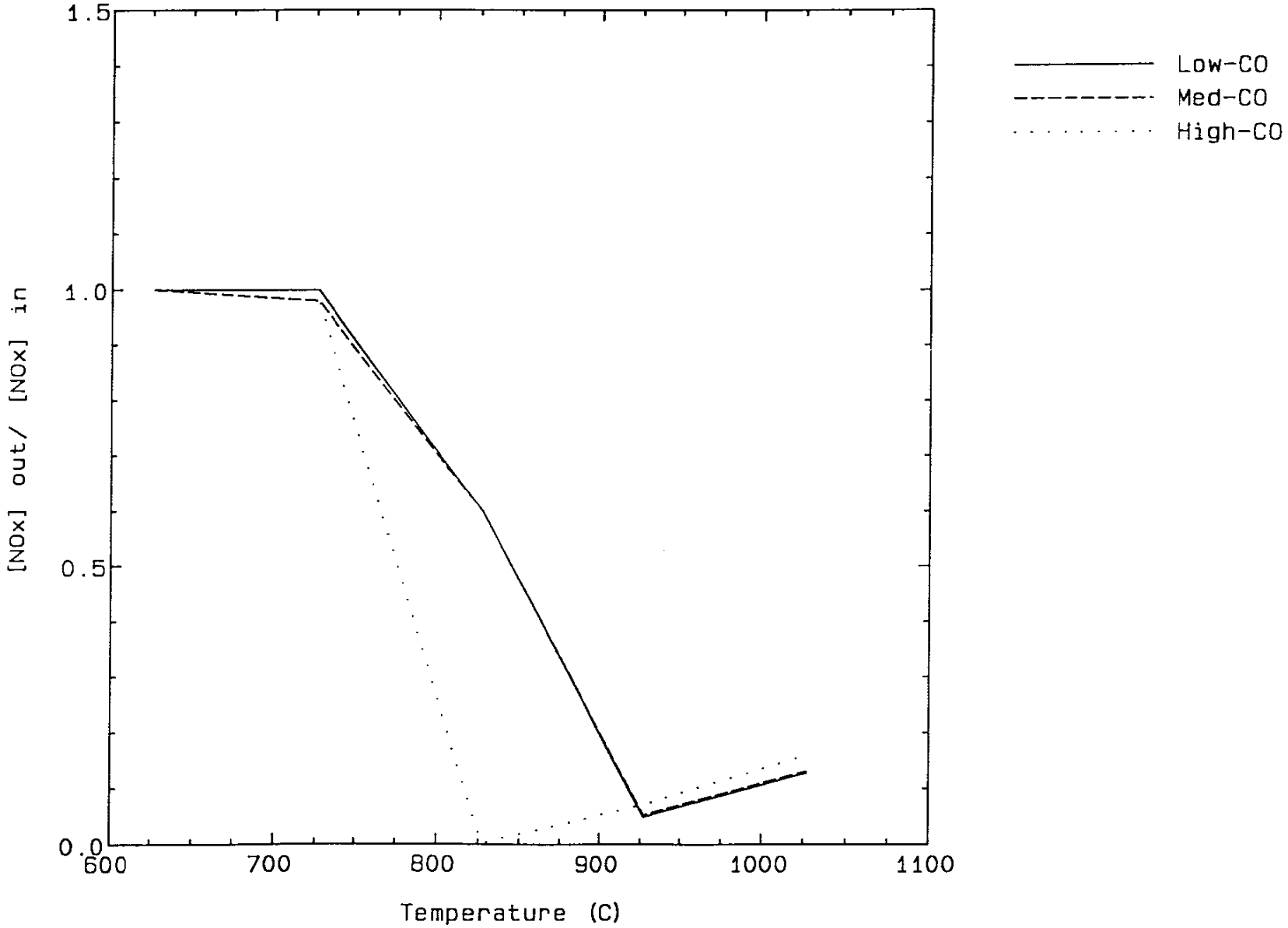

Figure 16. Calculated NO_x reduction efficiency as a function of temperature for selected initial condition: 5% O_2, 5000 ppm NO, HNCO/NO = 2. Initial CO conditions selected include low CO = 200 ppm, medium CO = 1000 ppm, and high CO= 5000 ppm.

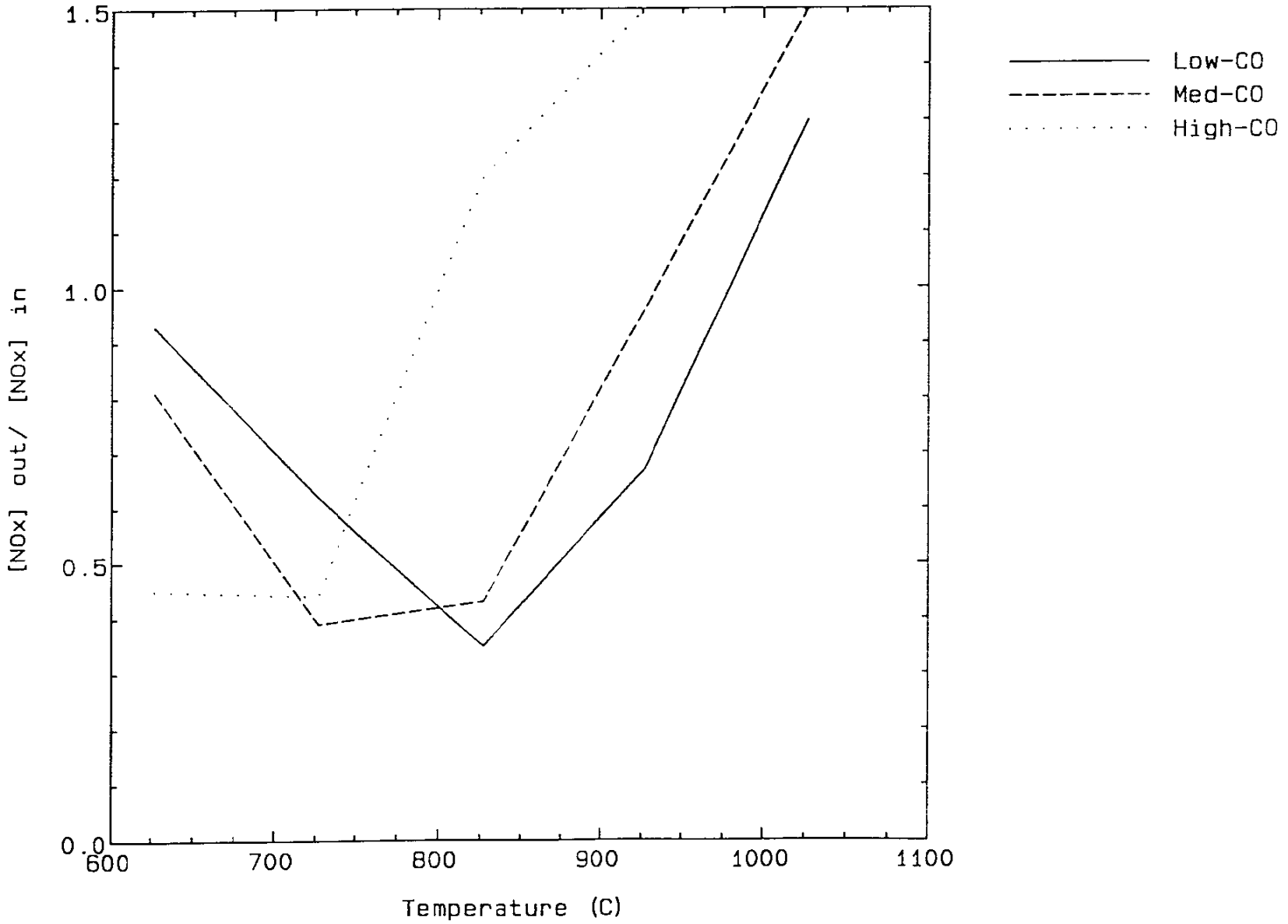

Figure 17. Calculated NO_x reduction efficiency as a function of temperature for selected initial condition: 10% O_2, 100 ppm NO, HNCO/NO = 1. Initial CO conditions selected include low CO = 200 ppm, medium CO = 1000 ppm, and high CO= 5000 ppm.

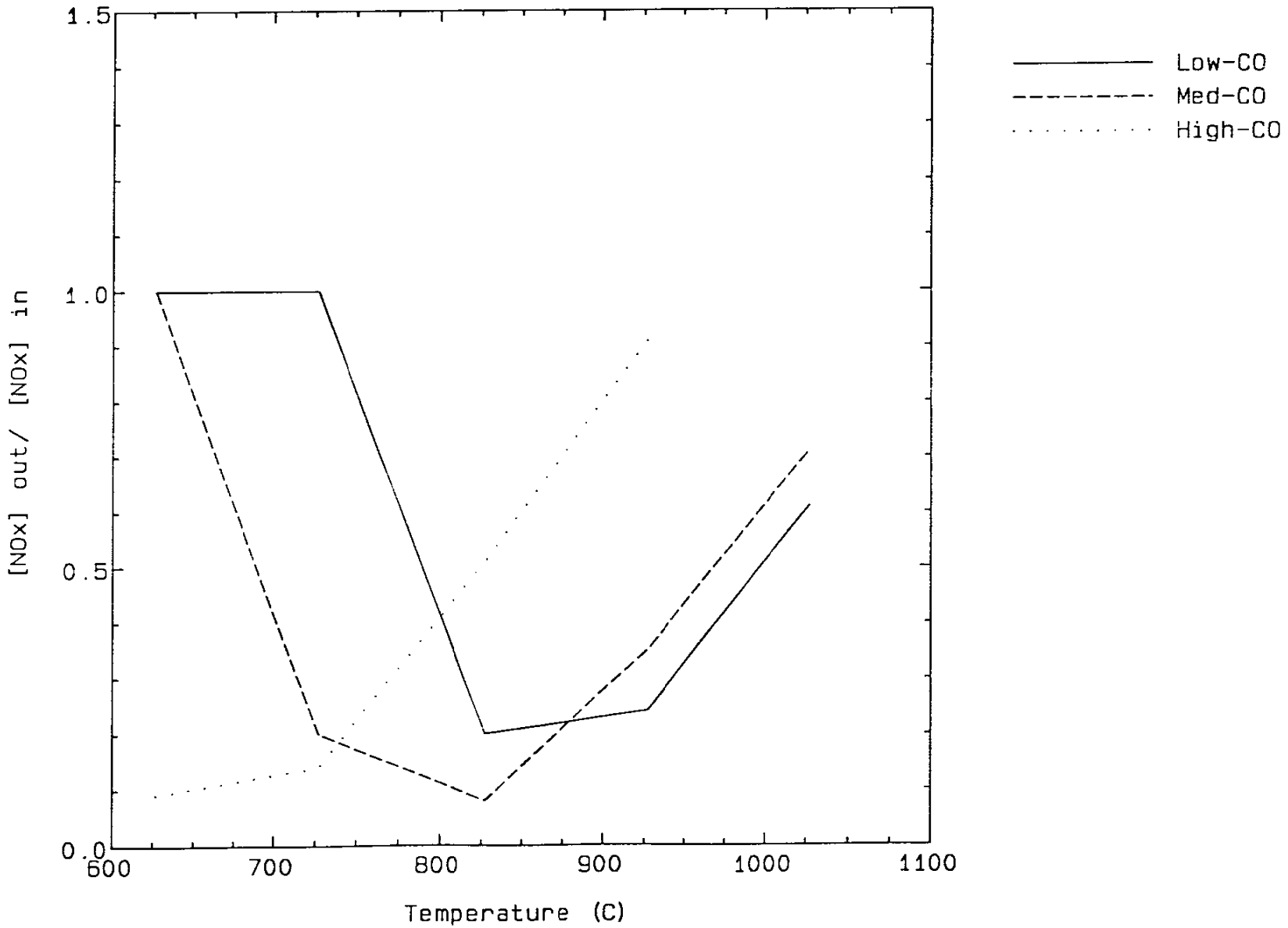

Figure 18. Calculated NO_x reduction efficiency as a function of temperature for selected initial condition: 10% O_2, 500 ppm NO, HNCO/NO = 1. Initial CO conditions selected include low CO = 200 ppm, medium CO = 1000 ppm, and high CO= 5000 ppm.

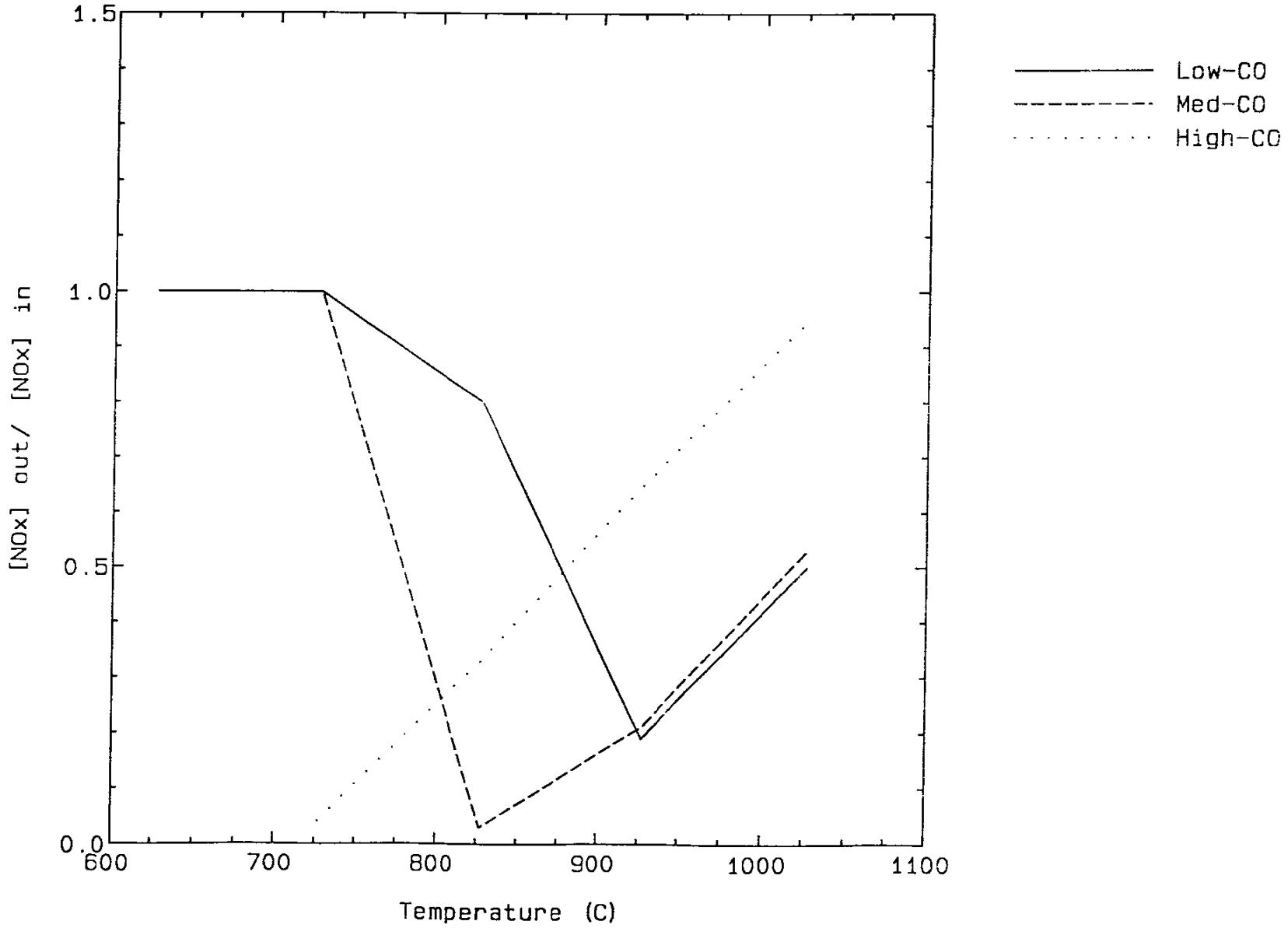

Figure 19. Calculated NO_x reduction efficiency as a function of temperature for selected initial condition: 10% O_2, 1000 ppm NO, HNCO/NO = 1. Initial CO conditions selected include low CO = 200 ppm, medium CO = 1000 ppm, and high CO= 5000 ppm.

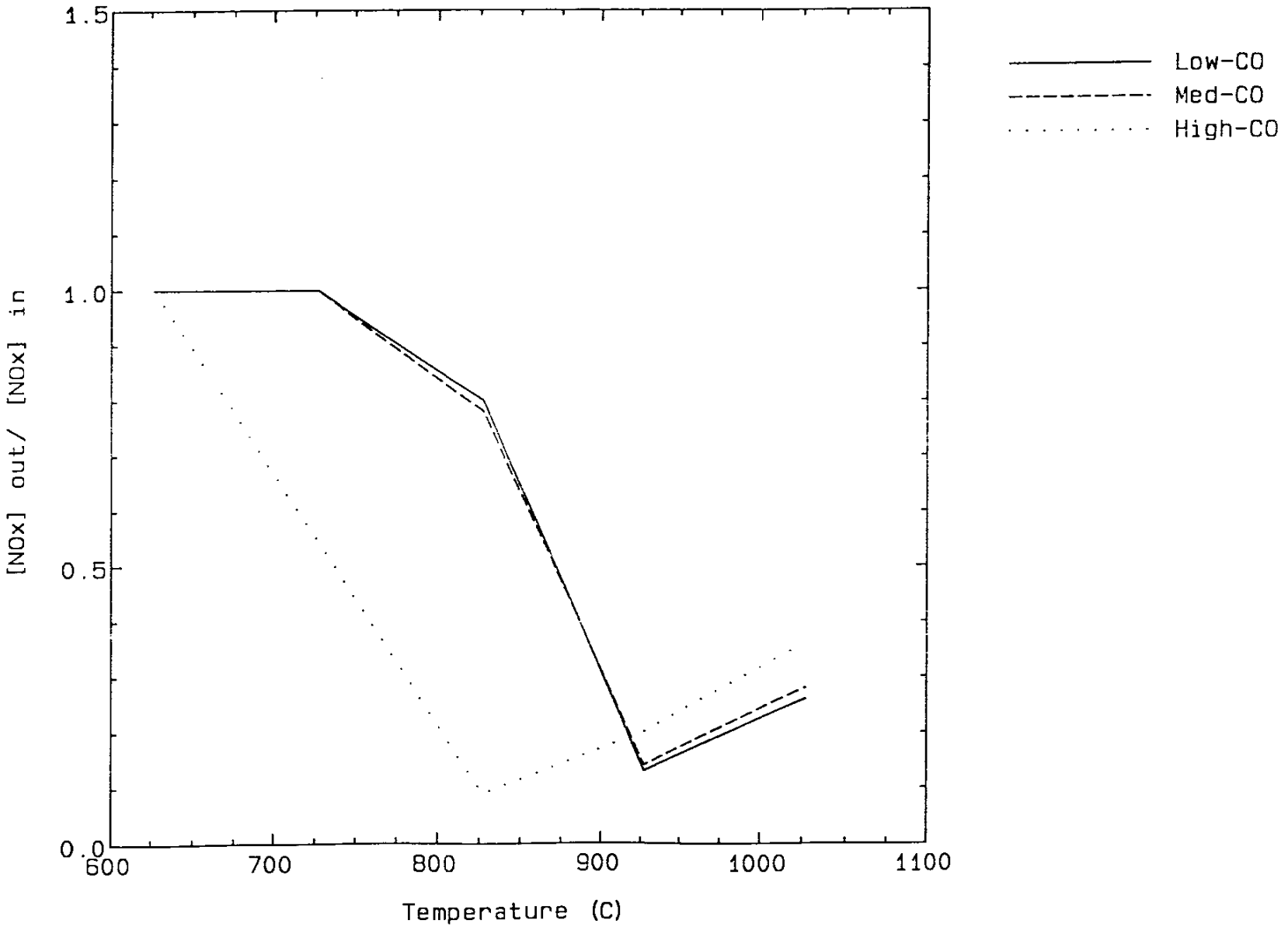

Figure 20. Calculated NO_x reduction efficiency as a function of temperature for selected initial condition: 10% O_2, 5000 ppm NO, HNCO/NO = 1. Initial CO conditions selected include low CO = 200 ppm, medium CO = 1000 ppm, and high CO= 5000 ppm.

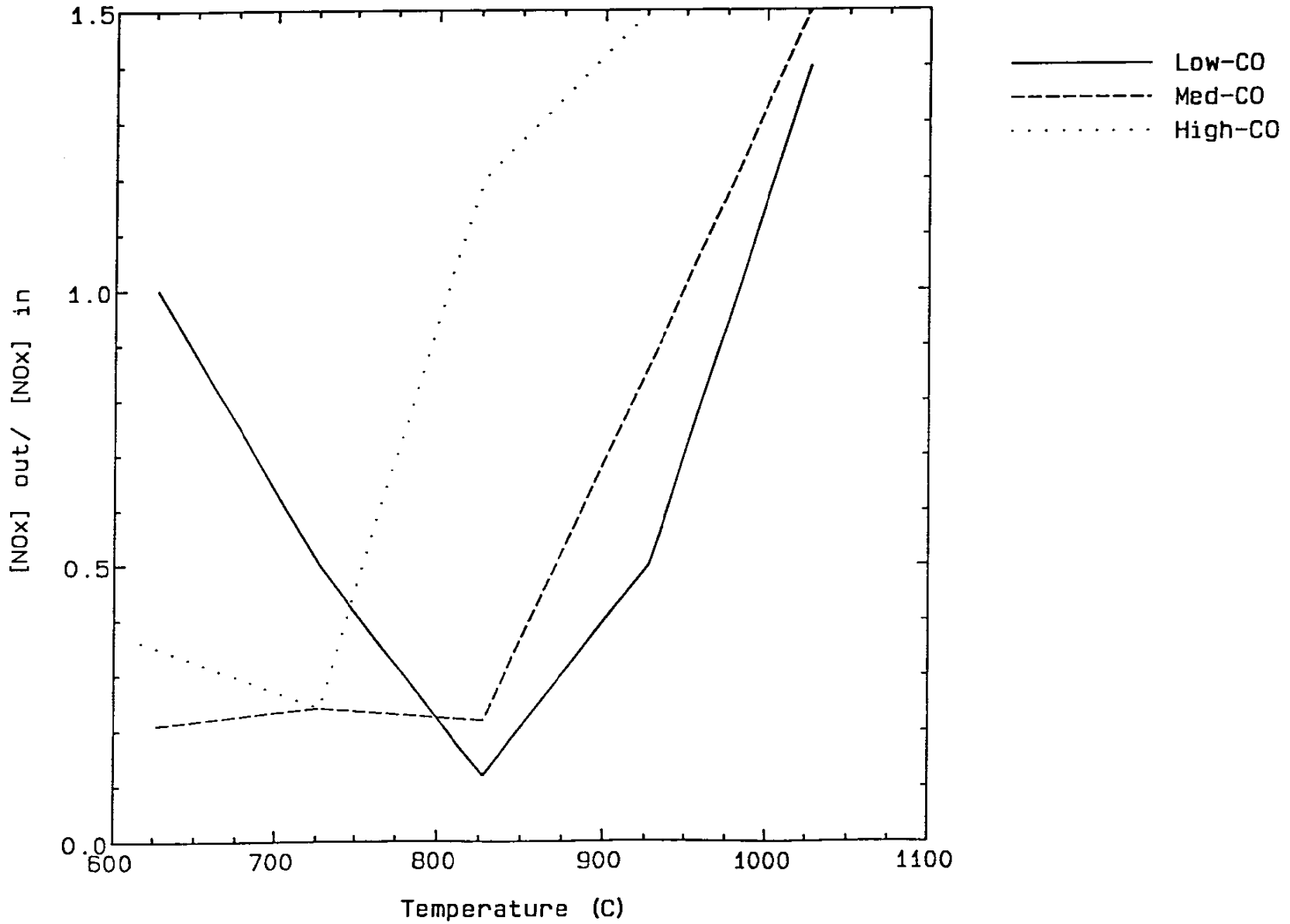

Figure 21. Calculated NO_x reduction efficiency as a function of temperature for selected initial condition: 10% O_2, 100 ppm NO, HNCO/NO = 2. Initial CO conditions selected include low CO = 200 ppm, medium CO = 1000 ppm, and high CO= 5000 ppm.

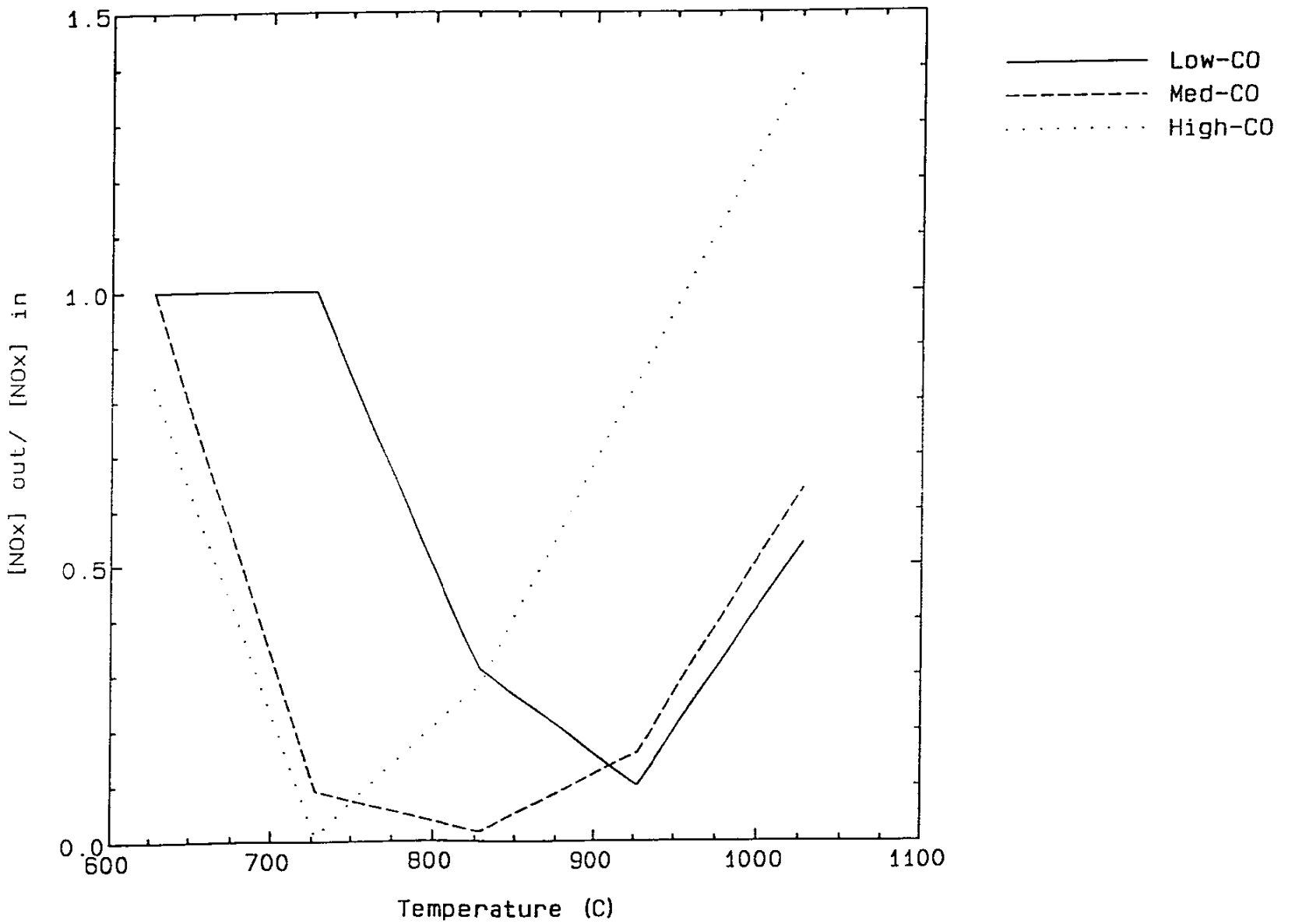

Figure 22. Calculated NO_x reduction efficiency as a function of temperature for selected initial condition: 10% O_2, 500 ppm NO, HNCO/NO = 2. Initial CO conditions selected include low CO = 200 ppm, medium CO = 1000 ppm, and high CO = 5000 ppm.

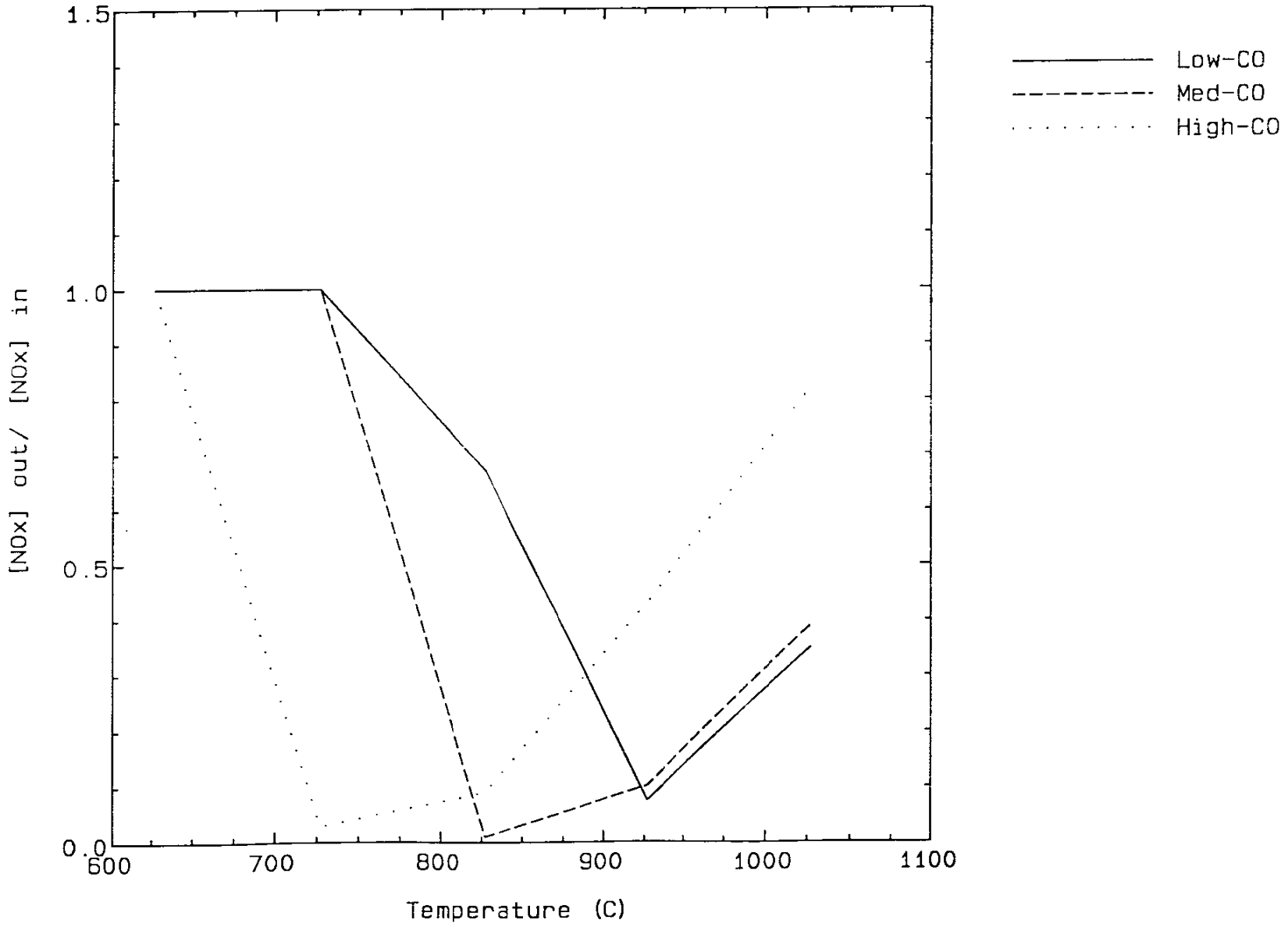

Figure 23. Calculated NO_x reduction efficiency as a function of temperature for selected initial condition: 10% O_2, 1000 ppm NO, HNCO/NO = 2. Initial CO conditions selected include low CO = 200 ppm, medium CO = 1000 ppm, and high CO= 5000 ppm.

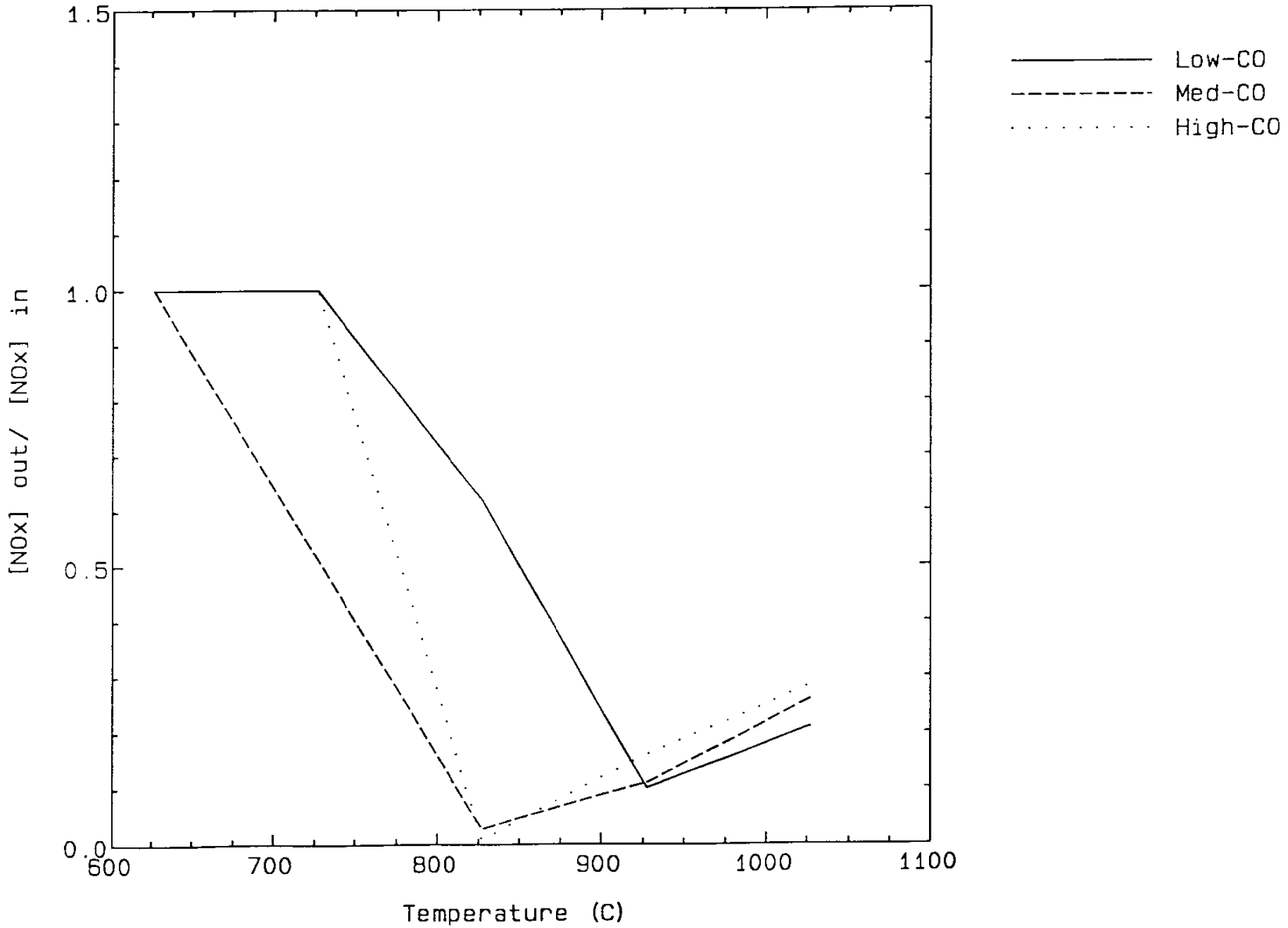

Figure 24. Calculated NO_x reduction efficiency as a function of temperature for selected initial condition: 10% O_2, 5000 ppm NO, HNCO/NO = 2. Initial CO conditions selected include low CO = 200 ppm, medium CO = 1000 ppm, and high CO = 5000 ppm.

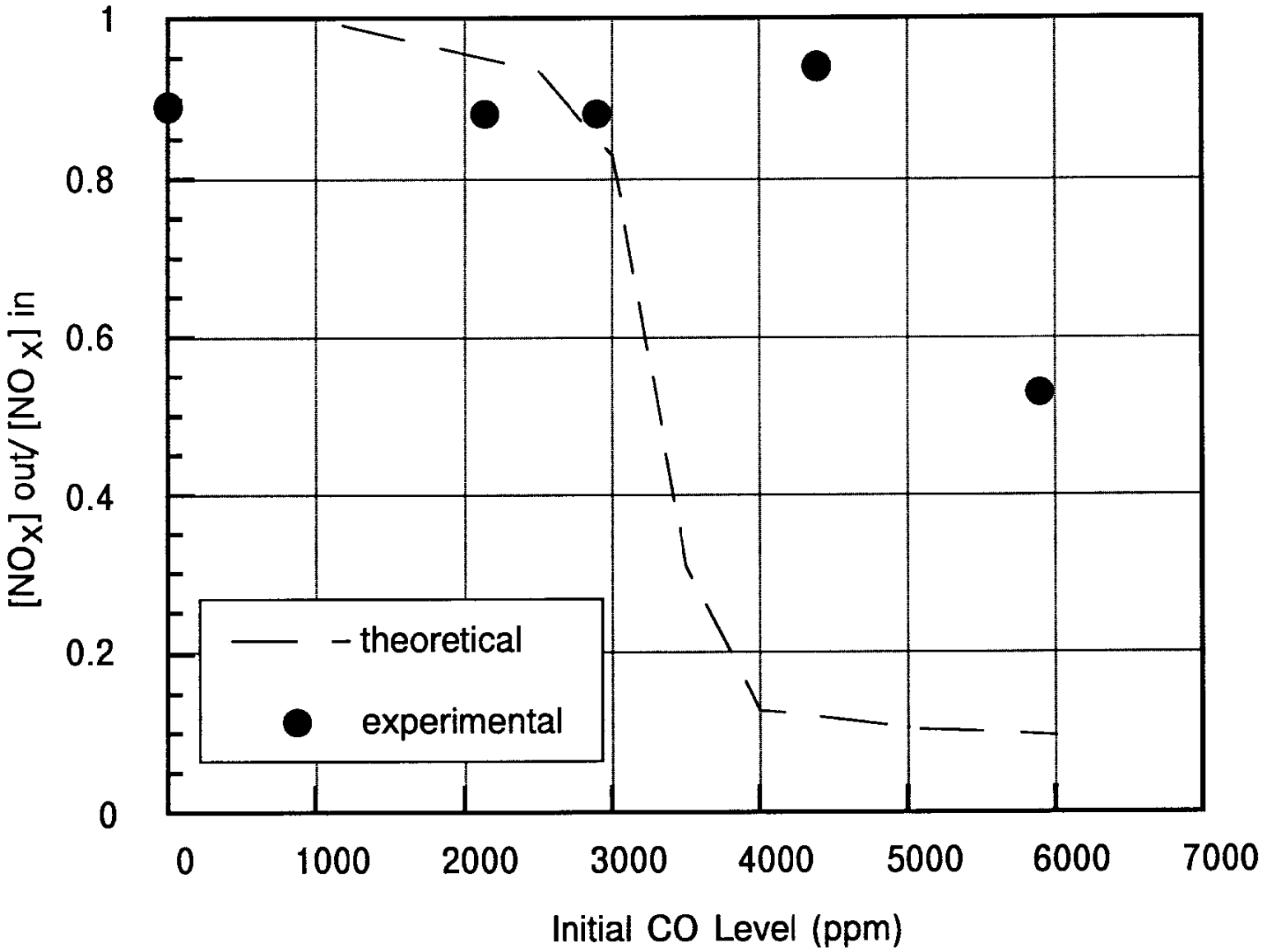

Figure 25. NO_X reduction as a function of carbon monoxide concentration at 635 C

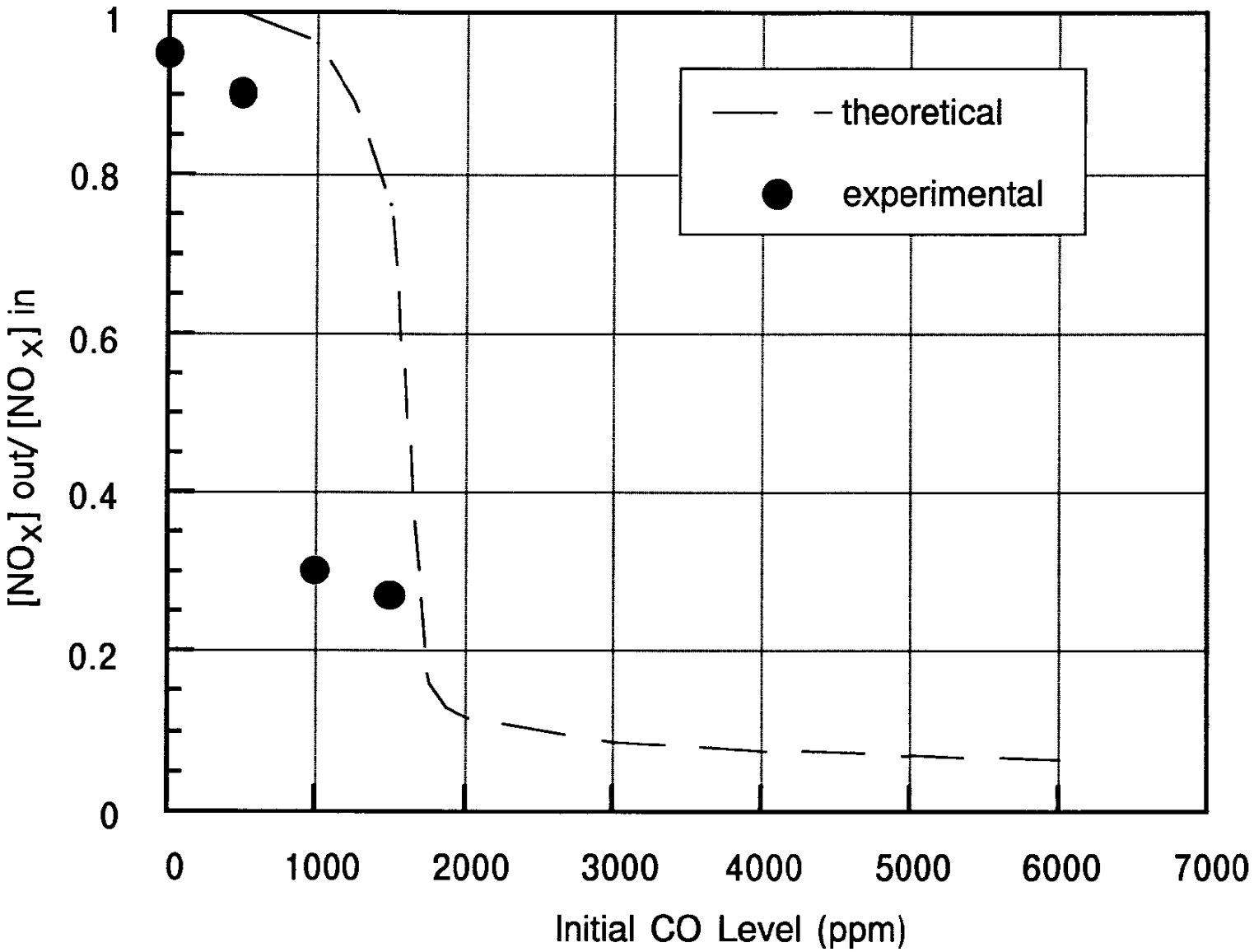

Figure 26. NO_x reduction as a function of carbon monoxide concentration at 680 C

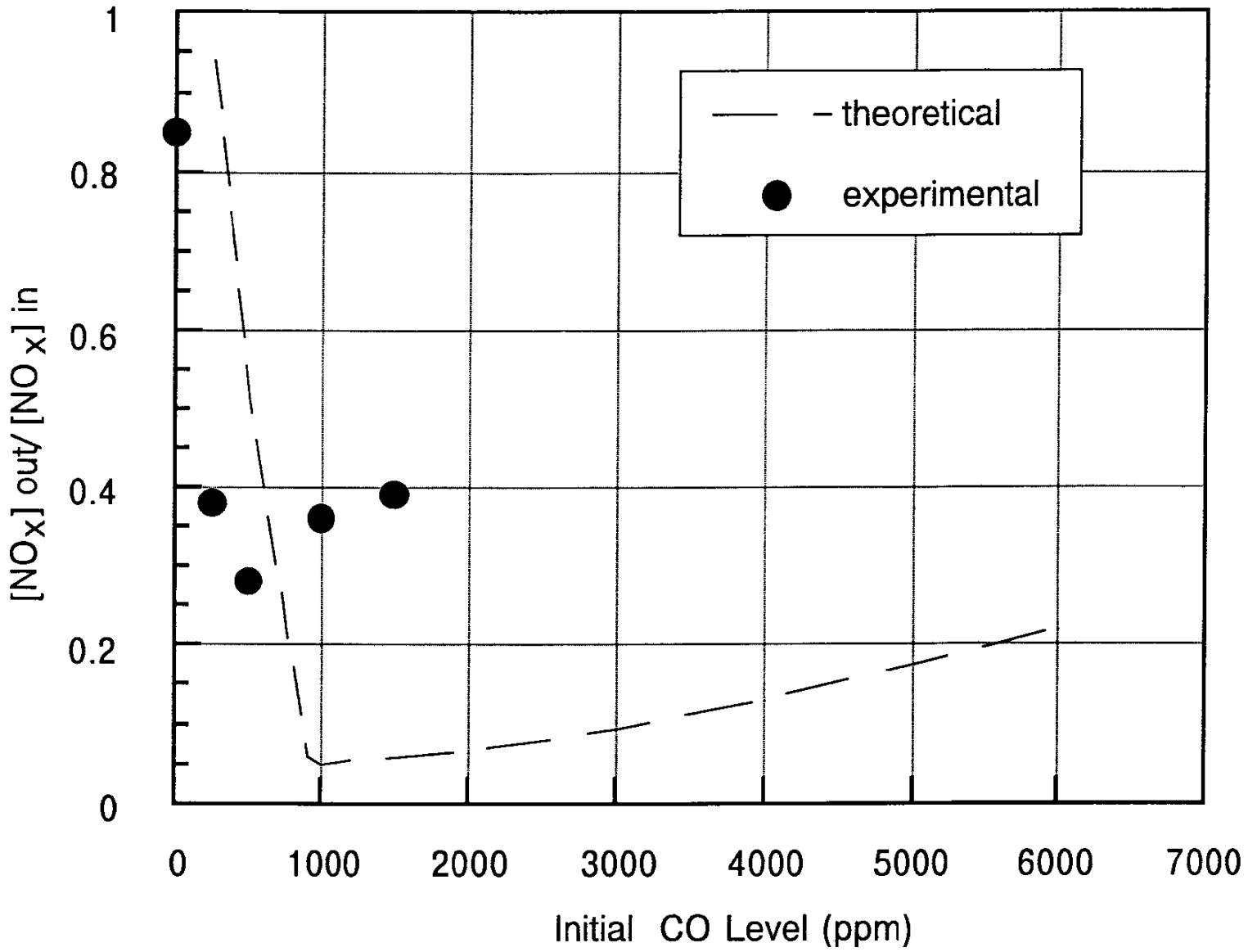

Figure 27. NO_X reduction as a function of carbon monoxide concentration at 760 C

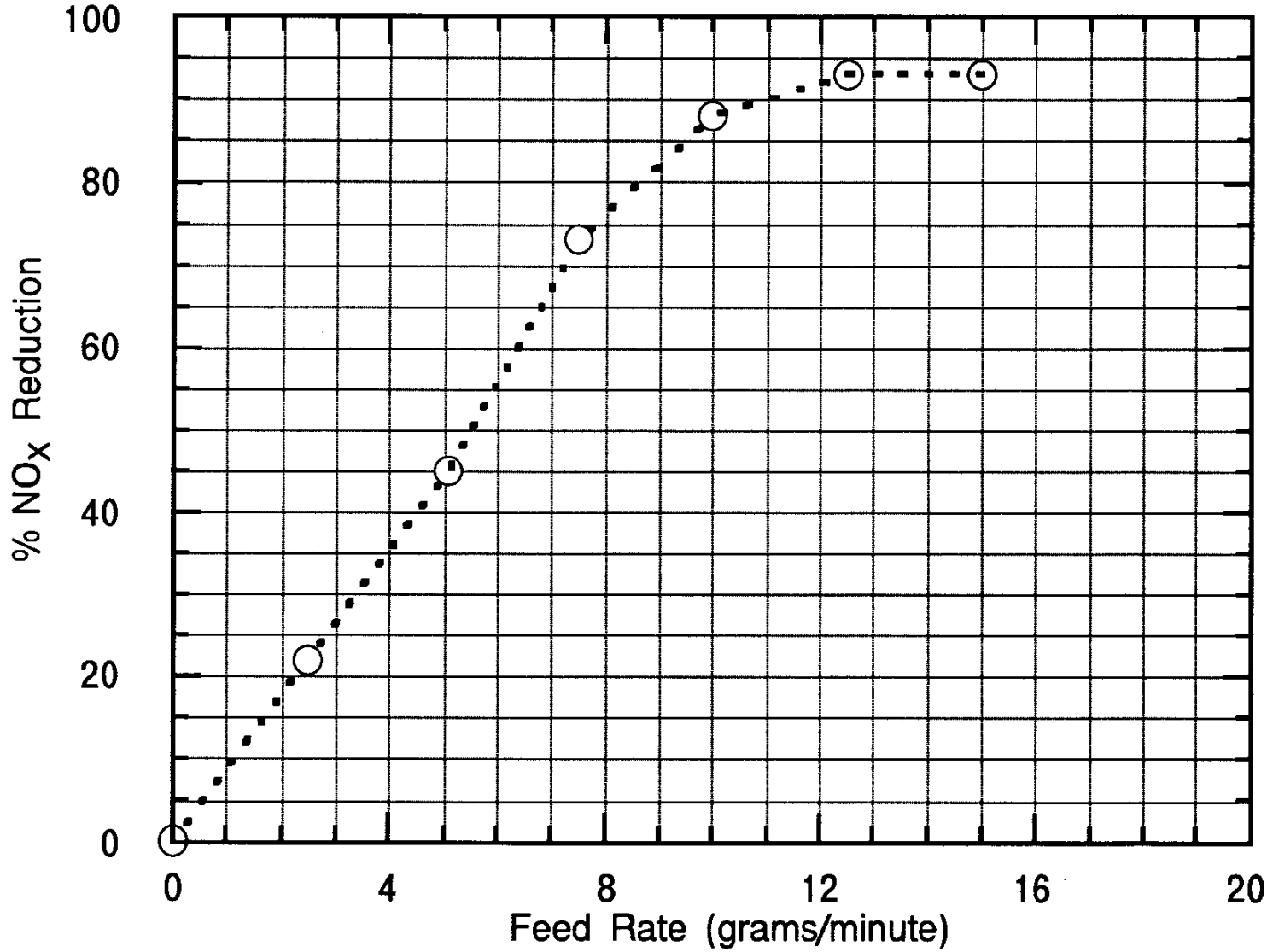

Figure 28. NO_X reduction as a function of CYA for a 37 kWatt genset operating at the following conditions: initial temperature = 550 C, initial NO_X = 1450 ppm, load = 100%, and co-injection of propane.

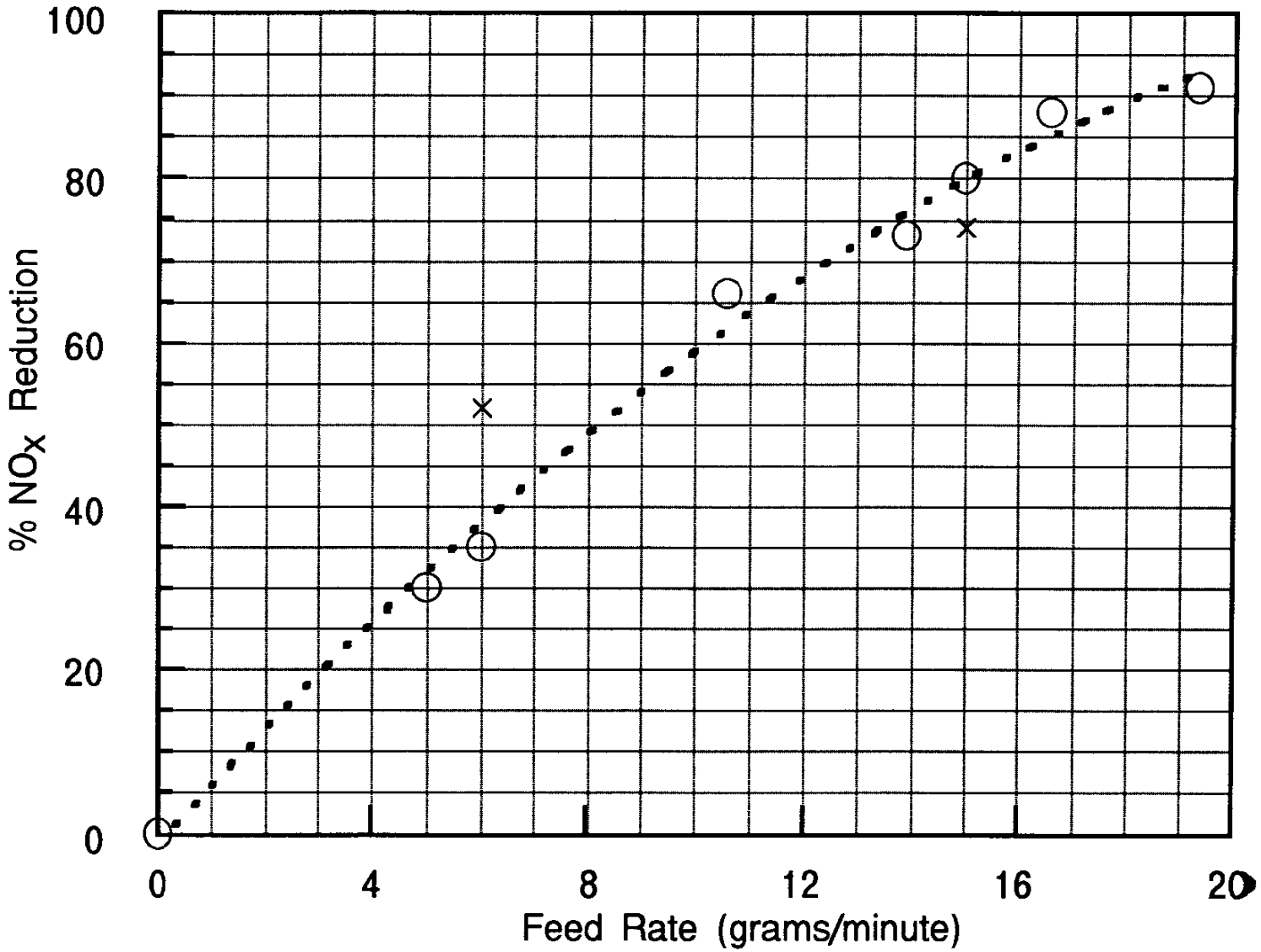

Figure 29. NO_X reduction as a function of CYA for a 100 kWatt genset operating at the following conditions: initial temperature = 427 C, initial NO_X = 820 ppm, load = 50 %, o = co-injection of propane, x = co-injection of diesel .

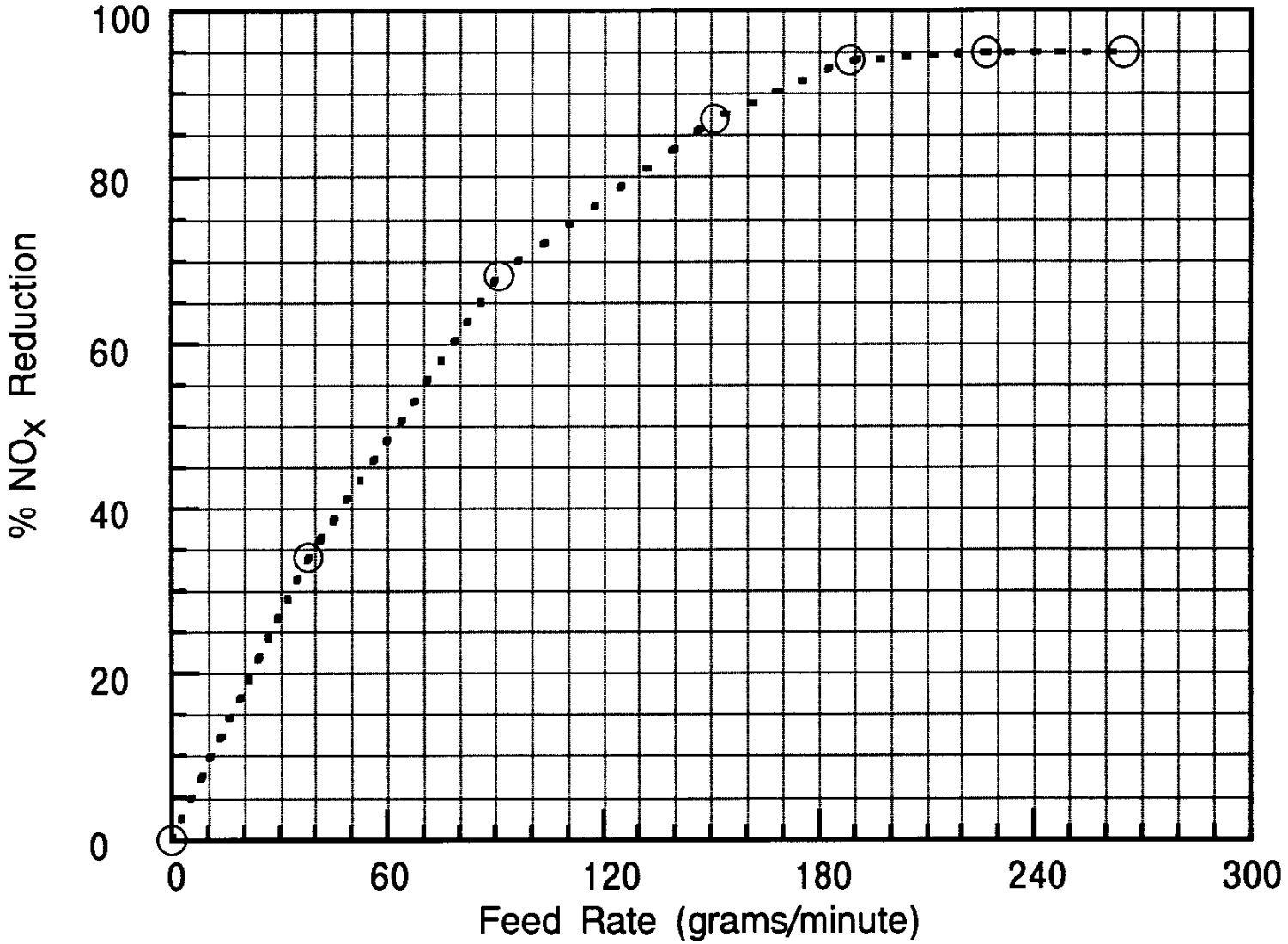

Figure 30. NO_X reduction as a function of CYA for a 1000 kWatt genset operating at the following conditions: initial temperature = 482 C, initial NO_X = 990 ppm, load = 80 %, and co-injection of propane.